NASA Contractor Report 201682

Estimating the Effects of the Terminal Area Productivity Program

David A. Lee, Peter F. Kostiuk, Robert V. Hemm,
Earl R. Wingrove III, and Gerald Shapiro
Logistics Management Institute, McLean, Virginia

Contract NAS2-14361

April 1997

National Aeronautics and
Space Administration
Langley Research Center
Hampton, Virginia 23681-0001

Estimating The Effects Of The Terminal Area Productivity Program

SUMMARY

We describe the methods and results of an analysis of the technical and economic benefits of the systems to be developed in the NASA Terminal Area Productivity (TAP) program. We developed a methodology for analyzing the technical and economic benefits of the TAP systems. To estimate airport capacity, the methodology uses inputs from airport-specific data on hourly weather, hourly operations counts, operating configurations, and mixes of transport aircraft types. The capacity model uses parameters that reflect the potential impacts of the TAP systems. The analytic approach takes the capacity estimates, calculates aircraft delays through a queuing model, and calculates the cost savings to airlines from reduced delays. The model analyzes the impact of advanced aviation technologies and changes in operating procedures on terminal area operations.

We establish preliminary estimates of the benefits of the TAP systems. As the TAP systems become better defined, more accurate and detailed analyses of the benefits of implementing these systems will be possible. Outputs from the analysis are preliminary estimates of the benefits of the TAP systems. Technical benefits include reductions in both means and variances of aircraft-minutes of delay; the latter reductions are important to airlines interested in schedule integrity. We estimate savings in airline operating costs from reduced delays.

The airport capacity estimates rest on three model pillars, two operational and one economic. For each of the two airports analyzed, these are a model of the airport capacity as a function of weather conditions, with parameters that can be adjusted to reflect impacts of the TAP technologies; a model of operations demand as a function of time; and a model of airline operating costs.

We applied the analytic method to Boston's Logan International (BOS) and Detroit's Wayne County (DTW) airports. Tables 1 through 4 summarize the key aircraft delay results. For each selection of TAP systems, airport capacity and the resulting delays were calculated and the airline cost savings computed. Tables 1 and 2 show the estimated annual aircraft delays for BOS and DTW for selected years, with and without the TAP systems. The estimates indicate a sharp increase in delays through the year 2015, as demand grows steadily and capacity increases are limited. There are sizable delay reductions from the TAP systems, as much as 50 percent from all TAP

systems operating at BOS in 2015. Table 3 shows the estimated cost of the baseline delays, based on estimates of aircraft operating costs and the mix of aircraft now flying into those two airports. An upper and lower bound on delay costs is provided to account for the uncertainty in where the delay is incurred (such as on the ground or while airborne). To quantify the impacts of some of the individual TAP systems, we defined three combinations of TAP systems. These are labeled TAP 1, TAP 2, and TAP 3.

TAP 1. The first TAP increment, Reduced Spacing Operations (RSO) includes the Aircraft Vortex Spacing System (AVOSS) with wake vortex sensors. We expect these elements to reduce the arrival separations currently maintained to avoid wake vortex threats.

TAP 2. The second TAP increment, Low Visibility Landing and Surface Operations (LVLASO) includes GPS precision landing capability plus cockpit taxi maps and sensor systems necessary to reduce arrival runway occupancy time during instrument meteorological conditions by 20 percent.

TAP 3. The third TAP increment, Advanced Traffic Management Center (ATM) includes integrated CTAS/FMS (Center TRACON Automation System/Flight Management System). Integration assumes two-way CTAS/FMS data linking. In the TAP 3 increment, CTAS would be operating "closed loop" with the current flight plans of individual aircraft. Moreover, the FMS capability provides high confidence that the plans will be carried out as described. Flight plan revisions will be communicated both ways in real time. The parametric result will be reduced uncertainty about aircraft status and intent that permits reducing Instrument Flight Rule (IFR) separations to near Visual Flight Rule (VFR) distances.

Table 1. Annual Aircraft Arrival Delay at BOS (Millions of Minutes)

Technology State	1993	2005	2015
Current	5.5	6.8	12.2
TAP 1	–	5.9	10.8
TAP 2	–	4.8	8.9
TAP 3	–	2.1	4.2

Table 2. Annual Aircraft Arrival Delay at DTW (Millions of Minutes)

Technology State	1995	2005	2015
Current	1.1	1.6	2.8
TAP 1	–	1.5	2.6
TAP 2	–	1.4	2.0
TAP 3	–	1.1	1.4

Table 3. Annual Aircraft Delay Costs (1993 $ Millions)

Airport	1993 ($)	2005 ($)	2015 ($)
Boston, upper bound	161	197	354
Boston, lower bound	90	110	198
Detroit, upper bound	37	55	95
Detroit, lower bound	21	31	53

The analysis leads us to conclude that implementing the TAP technologies will lead to substantial savings at BOS and DTW, although the amounts differ. Moreover, there are substantial benefits from each of the TAP technologies, as shown in Table 4.

Table 4. Present Value of TAP Benefits (1993 $ millions)

Airport	TAP increment 1 ($)	TAP increment 2 ($)	TAP increment 3 ($)	Total ($)
Boston, upper bound	165	236	542	937
Boston, lower bound	92	129	302	523
Detroit, upper bound	24	62	70	157
Detroit, lower bound	14	35	39	88

One conclusion of the study is that, for values of miles-in-trail separations and runway occupancy times consistent with the best data we found, both must be reduced if the

benefits of either are to be realized. Benefits of reduced miles-in-trail separations can be enjoyed only so long as runway occupancy times do not become the binding constraint, and similarly there is little benefit from reduced runway occupancy time if separations are not reduced. For this reason it is difficult to separate the benefits of RSO's reduced separations from the benefits of LVLASO's reduced runway occupancy times.

We also find that additional data collection would benefit our analysis.

Contents

FIGURES

TABLES

Chapter 1
Overview

This section provides background information on the NASA Terminal Area Productivity (TAP) research program. It sets out the objectives of the study, and briefly describes the approach developed to meet them.

TERMINAL AREA PRODUCTIVITY RESEARCH PROGRAM

The goal of the TAP research program is to safely achieve visible flight rule (VFR) capacity in instrument flight rule (IFR) conditions. In cooperation with the Federal Aviation Administration (FAA), NASA's approach is to develop and demonstrate airborne and ground technology and procedures to safely reduce aircraft spacing in terminal areas, enhance air traffic management and reduce controller workload, improve low-visibility landing and surface operations, and integrate aircraft and air traffic systems. By the end of the decade, integrated ground and airborne technology will safely reduce spacing inefficiencies associated with single runway operations and the required spacing for independent, multiple-runway operations conducted under instrument flight rules.

The NASA TAP program consists of four major program elements: Air Traffic Management (ATM), Reduced Spacing Operations (RSO), Low Visibility Landing and Surface Operations (LVLASO), and Aircraft/ATC System Integration. The ATM element builds on the Center TRACON Automation System (CTAS) Program currently being supported under the NASA base program and the FAA Terminal Air Traffic Control Automation (TATCA) Program. The RSO element focuses on building systems to reduce current aircraft spacing standards in terminal areas. LVLASO concentrates on developing technologies to cut delays on the ground during periods of poor visibility.

The fourth element of TAP, Aircraft/ATC Systems Integration, focuses on ensuring that the various systems developed under the other elements fit consistently into the overall system. The goals of this element are threefold: (1) Ensure coordination and integration between airborne and ground-side elements; (2) provide flight facility support; and (3) develop and maintain the systems focus with technology impact and cost-benefit analysis. This study was performed as part of the Aircraft-ATC Systems Integration element.

Each of the three research elements contains several projects. The most authoritative information about project products, milestones, and budgets is found in the Level 3 element program plans. NASA briefing material and interviews with NASA personnel augment the information from the Level 3 plans.

Tables 1-1 through 1-3 list the three TAP elements and projects along with supplemental information on technology content. The firmness of the projects varies considerably. Some projects such as lidar and radar vortex sensors are well-defined, while others such as those in LVLASO, RSO information for lateral spacing, and RSO CTAS/FMS integration are periodically revised, removed, and reinstated.

Table 1-1. Reduced Spacing Operations

Technology Program Area	Technology Products
Wake Vortex Systems	• Aircraft Vortex Spacing System (AVOSS) • Lidar Wake Vortex Sensor • Radar Wake Vortex Sensor • Demonstrated AVOSS prototype including integration of wake vortex prediction and sensing, weather, and aircraft information
Center TRACON Automation System Compatible Flight Management System Development (CTAS Compatible FMS)	• Increasingly comprehensive simulations of integrated CTAS/FMS operations • Flight tested full CTAS coordinated with FMS
Airborne Information for Lateral Spacing (AILS)	• Techniques to improve navigation precision on closely spaced parallel approaches • Conflict alerting, detection, and appropriate displays • Air/ground information technologies • Airborne flight test of the Improved Navigation Performance (INP) subsystem

Table 1-2. Low Visibility Landing and Surface Operations (LVLASO)

Technology Program Area	Technology Products
Reduced Runway Occupancy Time	• Roll Out & Turn Off system (ROTO) • Enhanced ROTO/DGPS-based landing system • ROTO & landing system requirements
Efficient and Safe Surface and Tower Guidance	• Taxi Navigation and Situation Awareness system (T-NASA) • 3-D auditory display for blunder detection and avoidance • Recommended crew procedures and air traffic management interface
Terminal Area Systems Integration /Evaluation	• Required navigation performance (RNP) for ROTO& surface operations • Dynamic Runway Occupancy Measurement System (DROMS) • Integration of Surface Management Advisor/Guidance & Control/Information presentation

Table 1-3. Air Traffic Management

Technology Program Area	Technology Products
Center TRACON Automation System/Flight	• Data exchange, fusion, and sharing techniques
Management System Development (CTAS/FMS Integration)	• FMS operations in the ARTCC for descents • FMS operations in the Terminal Radar Approach Control area • Field test of full CTAS/FMS scenario
Dynamic Routing	• CTAS automation tools for efficiently rerouting aircraft
Precision Approach to Closely Spaces Parallel Runways (PACSPR)	• CTAS Final Approach Spacing Tool (FAST) support for offset approaches
Dynamic Spacing	• CTAS/FAST integrated with AVOSS and DROM

At completion of TAP research and development in 2000, the technology requirements will be established by analysis and testing (validation). Hardware and software feasibility will be demonstrated by integrated tests (demonstration). The next phase of TAP development varies with the technology. Wake vortex sensors and other R&D hardware will require engineering and manufacturing development, probably by the FAA, while software products like CTAS upgrades may need no further development. (Some modifications of software will be required to meet FAA reliability and hardening standards.) Suites of commercial off-the-shelf hardware, like flight management systems and data links, may need no further development, but will require purchase or upgrading by individual airlines. TAP product categories consist of:

- algorithms and software that can be installed in existing FAA and aircraft systems,
- validated specifications supported by feasibility demonstrations for hardware to be further developed and purchased by the FAA, and
- specifications and recommendations for new or modified commercial off-the-shelf avionics to be purchased by the FAA and aircraft owners.

Objectives of this Study

This study aims to provide the analysis tools needed to estimate the potential impact and benefits of the systems under development in the NASA TAP program. The basic approach to the analysis is straightforward:

1. Quantitatively confirm that weather is the primary cause of reduced capacity and delay at the study airports.
2. Quantify the major weather patterns at the study airports.
3. Identify those weather conditions and airports at which the TAP systems may provide benefits.
4. Develop the analysis method and estimate the potential impacts of TAP on operations at the first two airports of interest.

This report summarizes the results of this analysis and describes the method used to quantify the benefits of the TAP systems. The method can be used to analyze other terminal area issues, such as changes in regulations or alternative operating procedures. We applied the method to analyses of Boston's Logan International Airport (BOS) and Detroit's Wayne County International Airport (DTW).

The TAP systems are designed to enable airports to operate in poor weather with the same efficiency that they operate in good weather. Poor weather limitations derive from the need for air traffic controllers to operate under instrument flight rules maintaining constant positive control of aircraft separations as opposed to sharing the responsibility with the pilots as is done in good weather under visual flight rules. The quality of aircraft data available to controllers and limits on human ability to manage multiple aircraft safely in poor weather result in conservative aircraft spacing and lower landing and takeoff rates. The TAP systems provide improved data and automation aids to help the controllers and the pilots operate at higher rates in poor weather. Consequently, this report begins with an extensive discussion of how weather affects airport operations and specifically arrival delays.

This study concentrated on arrival delays for two reasons: First, for many days on which study airports have significant arrival delays, the models indicate that departure capacity is not reduced as seriously as arrival capacity. Second, while it seems reasonable in this initial study to assume that the time-phasing of arrival demand generally follows the standard pattern for a given day, that assumption may not be reasonable for departure demand. Significant arrival delays seem certain to alter the time phasing of departure demand; on bad days, most arrivals will experience significant delays. Estimating departure delays even at a single airport, requires a model of the interaction between delayed arrivals and subsequent departures. A multi-airport network analysis is required to estimate properly the propagation of delays throughout an aircraft itinerary.

Also, we believe that airline choices affect data on departure delays. For example, there is some anecdotal evidence that airplanes often push back from the gate even though the crews know they will not be able to take off immediately, so that FAA ground holds will not be charged to the airlines. Unfortunately, this practice also causes the ground hold to be recorded as taxi-out delay. Concentrating on arrival delays allows a cleaner, more reliable link between TAP technologies and benefits. The impact of this decision is some conservatism in the benefit calculations: None of the TAP systems will increase departure delays; most should reduce them.

Figure 1-1 summarizes the approach employed in this study. The analysis focuses on aircraft-minutes of arrival delay in the terminal area as the principal performance measure. Estimating delay requires calculating airport capacity, airport demand, and identifying relationships among capacity, demand, and delay. This study uses both a standard model and a newly developed model to estimate airport capacity as a function of weather and aircraft and air traffic control parameters. Airport tower records provide the required measures of demand. Future demand is forecasted with the pre-

dictions in the FAA Terminal Area Forecast (TAF). Two well-known queuing models generate delay statistics from the interaction of capacity and demand.

Figure 1-1. Overview of the Analysis Method

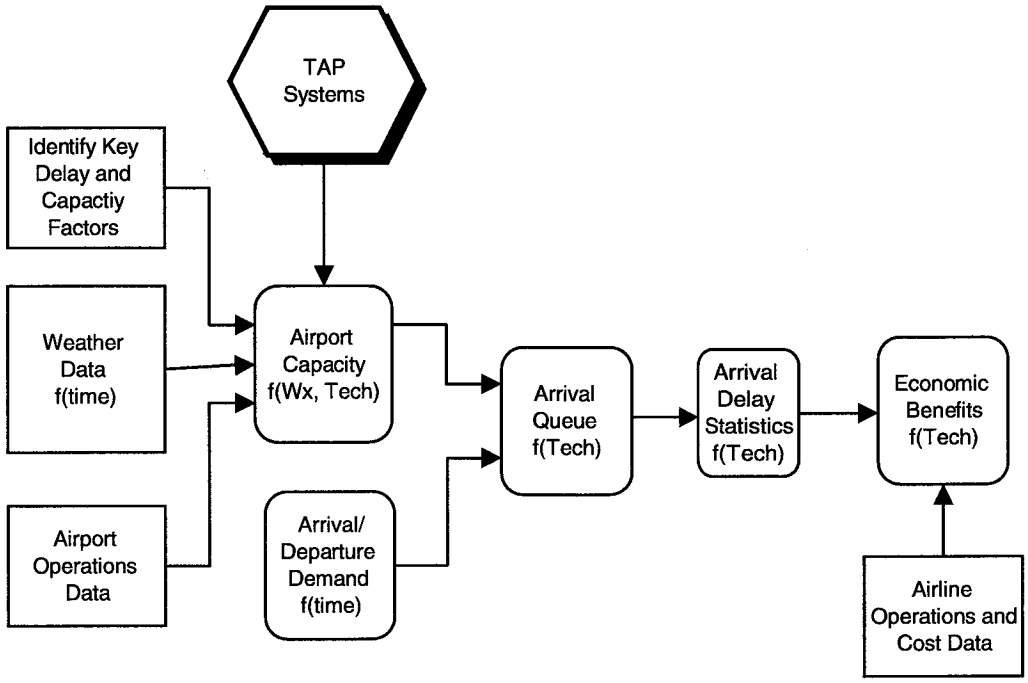

In the analysis, for given weather conditions at a specific airport, airport capacity is driven by the parametric variables in the capacity models. Those parameters, which include aircraft separation, approach speed, runway occupancy time, and uncertainties in approach speed and position are standard in capacity analysis and relate directly to controller behavior and equipment performance. The impacts of the TAP systems are crucial inputs in determining the correct parameters to be used in the capacity models.

The initial phase of the study focused on investigating the relationship among meteorological conditions, airport capacity, and arrival delay. This research included detailed hourly analysis of one year of weather and delay data for Boston and Detroit, plus detailed analyses for 1993 delays at eight other airports. This research provided a good understanding of the impact of weather on the capacity parameters in the capacity models, and confidence in the linkage of those parameters to arrival delay. That understanding was incorporated into a general runway capacity model and in airport-specific capacity models for Boston and Detroit.

The NASA TAP program documentation identifies the products of the technology projects. We worked with NASA to develop the relationships between those products and airport capacity parameters. Three ensembles of products for deployment in three TAP implementations were analyzed in order to estimate the individual effects of the TAP systems. Capacity model parameter values were estimated for a year 2005 baseline and for each TAP implementation. The three TAP implementations (TAP 1, 2, and 3) are cumulative in that TAP 2 adds to TAP 1 and TAP 3 adds to TAP 2.

Two steps were required to link delay reductions to changes in airline operating costs. First, we identified the elements of airline operating costs that are affected by terminal area delays. Second, we identified the relationship of those costs to the length of the delay. The effort required collecting and combining cost and operational data extracted from several sources and conducting literature research to provide insight into the nature of airline operating costs. With the cost per minute of arrival delay thus established, it is straightforward to calculate the benefits of the TAP systems from the increases in capacity and corresponding reductions in delay they provide.

This analysis aimed to estimate the potential benefits of implementing the TAP systems at two airports. The study did not address the technical feasibility of achieving the TAP program goals, and did not estimate the costs of developing or acquiring those systems.

Chapter 2
Characteristics of Weather and Delays at BOS and DTW

The first phase of the study examines the effects of weather on airport capacity and delay. Through a review of airport operations and their dependence on weather, we identified the crucial components that were required for estimating the potential effects of the TAP systems. The analysis of delay and weather patterns identifies those problems amenable to TAP, and provides an interesting overview of the challenges facing terminal area aircraft operations.

Definitions of Operating Categories at the Study Airports

Meteorological conditions are the chief determinants of terminal area capacity, once physical plant and procedures are fixed. While meteorological conditions vary continuously, an airport operates only in a finite set of configurations and under a finite set of ATC procedures, determined by meteorological conditions. This section describes the meteorological conditions categories.

The FAA defines two basic meteorological conditions: visual meteorological conditions (VMC) and instrument meteorological conditions (IMC). During VMC, flights may operate under either visual flight rules (VFR) or instrument flight rules (IFR). Under IMC, only IFR operations are allowed. The basic VMC/IMC distinction is universal: conditions are VMC if the ceiling (height above the surface of the lowest cloud layer that obscures 50 percent or more of the sky) is 1,000 feet or more, and the horizontal visibility at the surface is three miles or more.

Two subcategories of VMC are important for operations in the terminal area. When ceiling and visibility are sufficiently good, Terminal Radar Approach Control (TRACON) controllers will allow IFR flights to end with visual approaches. In this case, aircrews accept responsibility for maintaining safe separations between aircraft; landings are made under the direction of controllers in the tower cab, like in VFR approaches. Generally, aircrews are comfortable with closer spacings than the IFR minima when making visual approaches, so that terminal areas have their greatest capacity when meteorological conditions are above visual approach minimums. These minimums vary from airport to airport, and they are usually more restrictive than those for universal VMC. The two classes of VMC–i.e., VMC conditions under

which visual approaches are allowed, and VMC conditions under which they are not are sometimes called VFR1 and VFR2 conditions, respectively.

There are also sub-categories of IMC, related to different kinds of IFR operations. FAA procedures allow IFR approaches to be made in several ways. IFR approaches by air carriers at major U. S. airports are, however, usually made with an Instrument Landing System (ILS). Accordingly, the ILS ceiling and visibility categories are the most important sub-categories of IMC for air carrier operations in the U. S., and thus for airport capacity. Most airports use two categories (IFR1 and IFR2) to classify IFR operations, based on ceiling and visibility. Table 2-1 defines the four operating conditions for BOS and DTW.

Minimum conditions are also prescribed for IFR departures. The Federal Aeronautical Regulations (FAR) Part 91 prescribes minimum visibility of one statute mile for IFR departures by aircraft with two engines or less, and one-half statute mile for other aircraft. These overall minima are often superseded by airport-specific minima that may vary from runway to runway. For example, at Chicago O'Hare (ORD), IFR departure minima are 300 feet and one mile on runway 22R, and 500 feet and one mile on runway 36.

Table 2-1. Ceiling and Visibility for Operating Conditions at BOS and DTW

Airport	VFR 1		VFR 2		IFR 1		IFR 2	
	Ceiling Minimum (feet)	Visibility Minimum (miles)	Ceiling Minimum (feet)	Visibility Minimum (miles)	Ceiling Minimum (feet)	Visibility Minimum (miles)	Ceiling (feet)	Visibility (miles)
BOS	2,500	5.0	1,000	3.0	300	3.0	<300	<3.0
DTW	4,500	5.0	1,000	3.0	200	3.4	<200	<3.0

DELAY AND WEATHER DATA

The following subsections describe summary data on aircraft delay and weather patterns at Boston Logan and Detroit Wayne County airports. The delay data are based on the Airline Service Quality Performance (ASQP) data that record scheduled and actual times for departure and arrival for individual flights. Data for all of 1993 were collected and analyzed for this study. Data elements from other sources, once merged into the ASQP, provided additional information on delays by phase of flight.

Aircraft delay was divided into four phases of flight. Those delays are defined as follows:

- Taxi-in. actual taxi-in time minus the minimum time required to taxi
- Arrival. actual arrival time minus scheduled Official Airline Guide (OAG) arrival time
- Travel. actual gate-to-gate time minus scheduled (OAG) gate-to-gate time
- Airborne. actual airborne time minus planned airborne time.

The weather data used in this analysis were obtained from the National Climatic Data Center. Two types of data were used. First, we used the actual hourly weather reports for 1993 to correlate flight delays at the two airports with the ground weather reported on those days. Second, we analyzed hourly weather reports from 1961 to 1990 to provide a detailed description of the types of weather phenomena that occurred at the two airports. Those data also supply valuable information on the sources of inclemency that affect aircraft operations. The key weather variables most often used in this study are ceiling, visibility, wind speed, and wind direction. In addition, we used data elements describing ice and snow conditions, fog, haze, and thunderstorms to estimate how useful the TAP systems might be at increasing capacity at the study airports during IMC.

Delays and Weather at Boston

We obtained flight-by-flight data on delays at BOS for 1993. Two kinds of analyses of these data were performed: global statistical analyses, which give insights into the differing kinds of weather conditions that cause delays at specific airports, and time series analyses, which are used to develop airport capacity and delay models.

Figure 2-1 shows some average delays in four meteorological condition categories. The increase between VFR1 and VFR2 shows the effect at BOS of losing the ability to end IFR flights with visual approaches. The much greater increases associated with IMC (IFR1 and IFR2) reflect the fact that BOS loses the ability to operate key runways—4R/4L or 22L/22R—independently in IMC.

Figure 2-1. Average Delays by Operating Conditions, BOS Arrivals in 1993

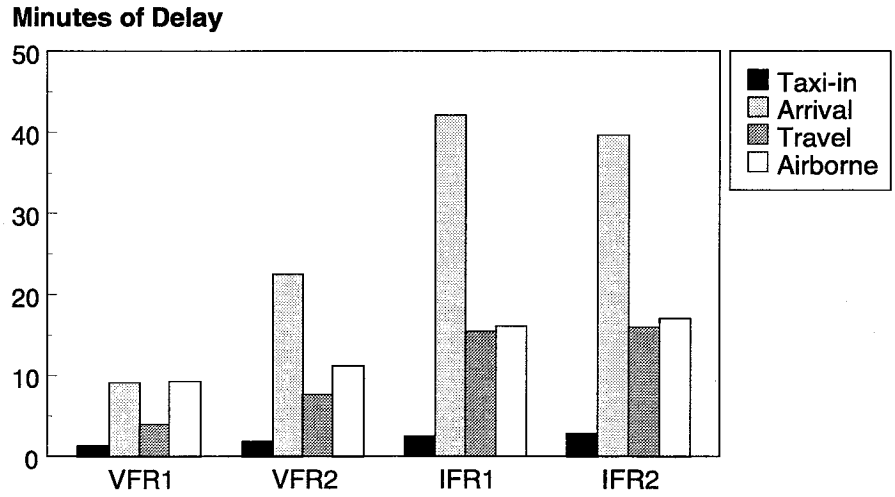

Figure 2-2 shows delays for four phases of flight by time of day for VFR1 flights arriving at BOS in 1993. The chart shows the importance of changes in hourly demands in determining delays, even controlling for weather conditions. At Boston Logan, the gradual increase in average delay for all flight phases over the course of the day is very noticeable. Another significant observation is that the sharp increase in arrival delay during IFR operating conditions is not matched proportionally by either travel or airborne delay. This demonstrates the impact of the FAA Estimated Departure Clearance Time (EDCT) program that holds aircraft on the ground at the departure airport when the demand-to-capacity ratio at the arrival airport is too unfavorable. The EDCT program explicitly trades airborne delays for gate holds in order to reduce the load on air traffic controllers and reduce operating costs to the airlines.

Figure 2-2. Delays by Phase of Flight and Time of Day, BOS VFR1 arrivals in 1993

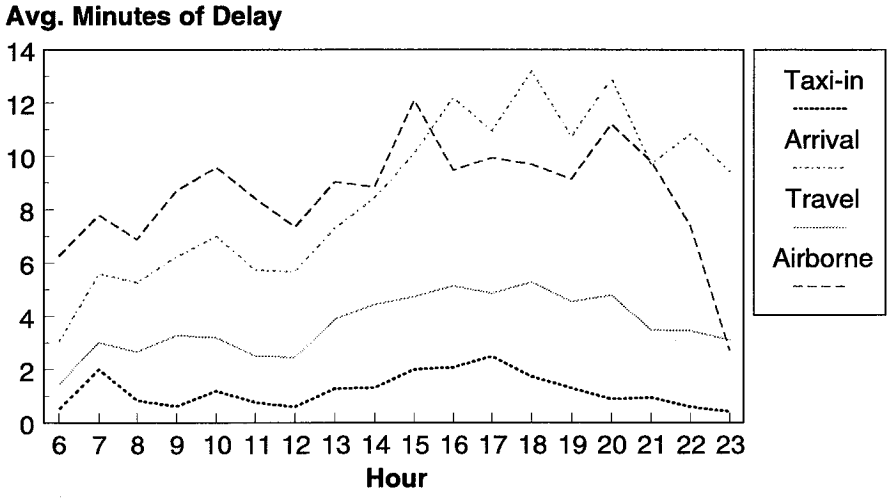

Table 2-2 shows how total delays were associated with meteorological conditions in 1993. These data show that the total delay in VMC is greater than the total in IMC, even though mean delays in IMC are much larger than mean delays in VMC. This occurs because a much greater percentage of the flights arrive during VFR; the total delay is larger even though the average delay per flight is much less.

Table 2-2. Total Delays at BOS in 1993 (in Thousands of Minutes)

Weather	Taxi-in	Airborne	Arrival	Travel
VFR1	97	656	649	184
VFR2	14	85	181	60
IFR1	4	28	79	28
IFR2	12	74	183	70
Total	130	854	1,119	452

Table 2-3 shows the frequency distribution of arrival delays, for four operating categories based on ceiling and visibility and for all flights. These data indicate that in VFR1, almost half the flights arrive early (i.e., reach the arrival gate ahead of their OAG schedule). In both IFR1 and IFR2, by contrast, nearly half the flights are more than half an hour late.

Table 2-3. Distribution of Arrival Delays at BOS in 1993 (by Meteorological Conditions)

Delay (minutes)	VFR1 (%)	VFR2 (%)	IFR1 (%)	IFR2 (%)	All Flights (%)
<0	49	31	17	18	45
0-5	15	12	8	8	14
5-10	11	10	9	7	11
10-15	7	8	7	6	7
15-20	4	6	6	6	5
20-25	3	5	5	5	3
25-30	2	4	5	5	2
30+	8	25	44	44	13

To understand the potential impact of TAP at Boston, we investigated the predominant weather conditions that affect airport operations. Figure 2-3 shows the percentage of time during important operating periods (6 a.m. to midnight) that specific ceiling and visibility conditions were present. At Boston, the definitions are VFR1, ceiling greater than 2,500 feet and visibility greater than 5 miles; VFR2, ceiling at least 1,000 feet and visibility at least 3 miles; IFR1, ceiling greater than 300 feet and visibility greater than 0.34 miles; IFR2, ceiling less than 300 feet or visibility less than 0.34 miles. The chart shows that IFR conditions occurred about 13 percent of the time during this 30-year period, with substantial variability across years.

Figure 2-3. Annual Operating Conditions at BOS

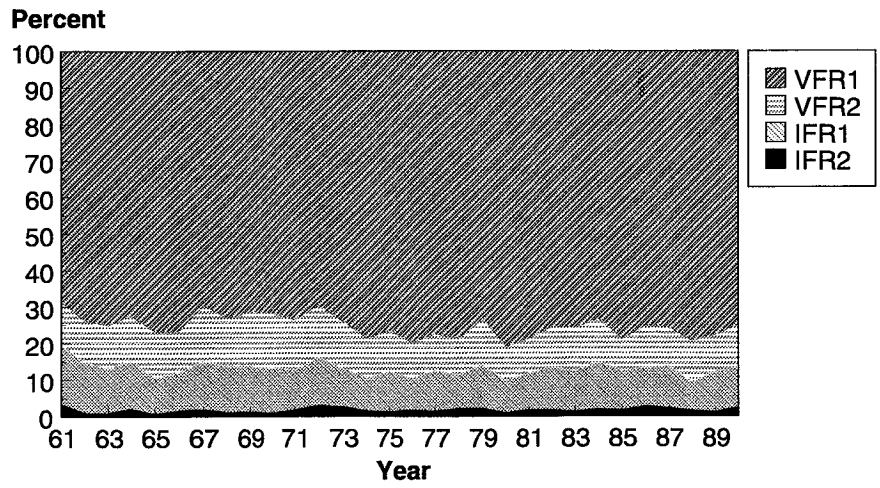

We next examined whether the weather conditions that produced the poor ceiling and visibility at BOS could possibly be overcome by systems under development in TAP. For example, the wake vortex detection systems and GPS landings could restore some of the capacity lost to poor visibility during haze and fog, but are not likely to be productive during severe thunderstorms or when runways are icy. Figure 2-4 shows how frequently specific weather conditions occurred during the four operating conditions. The results clearly demonstrate that the predominant causes of poor operating conditions during IFR are rain and fog. Consequently, there is reason to expect that successful implementation of some of the TAP systems could make a significant impact at BOS.

Figure 2-4. Boston Weather and Operating Mode

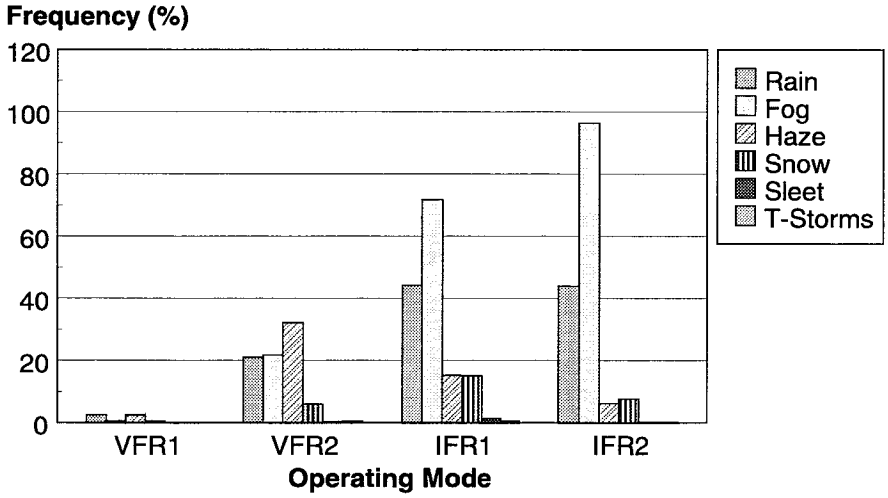

Another important factor in quantifying the benefits of advanced ATM systems is the correlation of arrival demand and weather at the airport. At many airports, demand varies markedly from hour to hour, and if poor weather occurs during a peak arrival period the delay impact is heightened. Figure 2-5 shows the hourly pattern of fog at BOS, again averaged over the 30-year period from 1961 to 1990. The pattern shows very clearly that fog is most common early in the morning, which coincides with one of the daily demand peaks. Figure 2-6 shows the hourly fluctuations in haze, which also coincides with morning rush periods.

Figure 2-5. Boston Fog by Hour

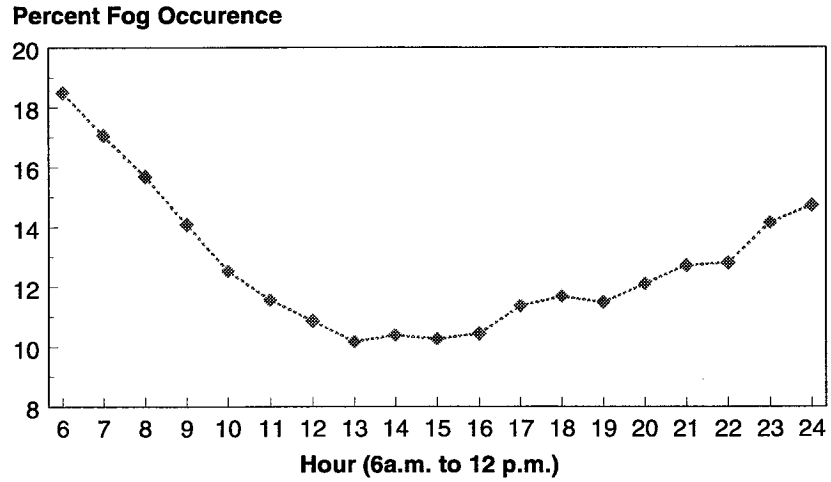

Figure 2-6. Boston Haze by Hour

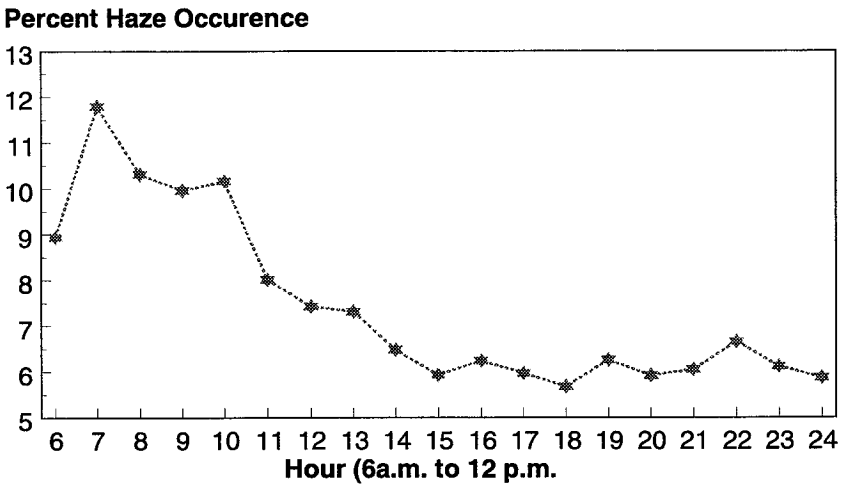

The weather data described in the charts above, combined with the sizable differences in delay by operating conditions, indicate that there is good potential for TAP technologies to improve capacity and reduce delay at Logan airport. Moreover, other analyses we completed showed conclusively that the correlation between operating conditions and arrival delay is very high. For nearly all the days analyzed, arrival delays were lowest during VFR1 and highest during IFR as defined by ceiling and visibility only. However, the analysis indicated other weather conditions that are

important to consider in addition to ceiling and visibility. About one-quarter of the 1993 VFR1 arrival delay at BOS occurred during times when ice was present on the runway. Less frequently, on other days, there is a sizable capacity loss when high winds come from particular directions. Therefore, any modeling of capacity and runway use at BOS must consider these other factors in addition to ceiling and visibility.

Delays and Weather at Detroit

We conducted a similar analysis to identify key weather and delay conditions at Detroit Wayne County Airport. The data in Figures 2-8 to 2-10 largely parallels the data for BOS and are provided for the reader's information. Figure 2-7 shows that IFR conditions occur 14.5 percent of the time at DTW, slightly more often than at BOS.

Figure 2-7. Annual Operating Conditions at DTW

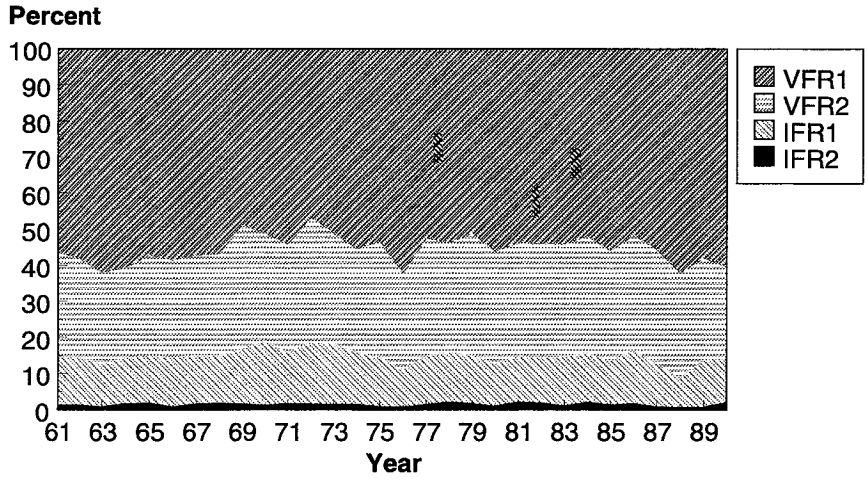

Figure 2-8. Detroit Weather and Operating Mode

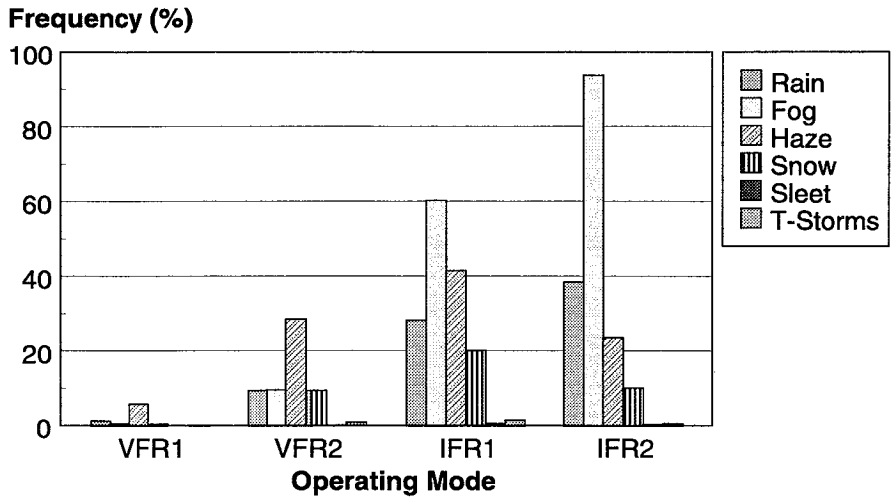

Figure 2-9. Detroit Fog by Hour

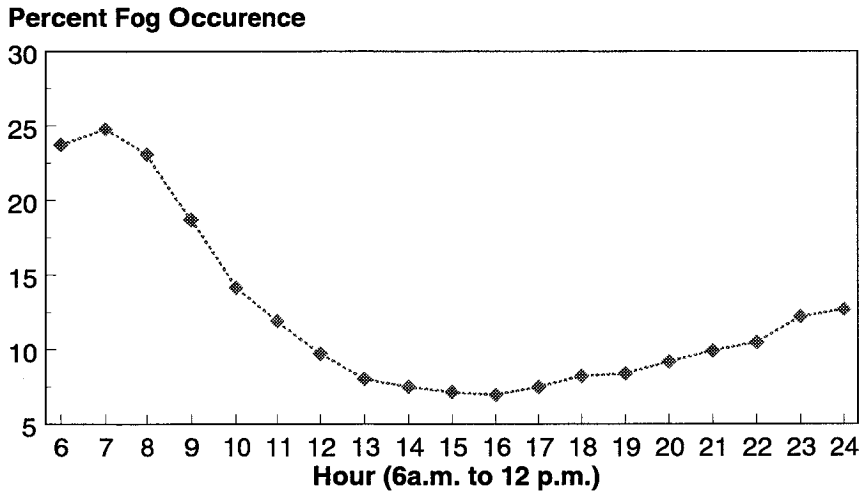

Figure 2-10. Detroit Haze by Hour

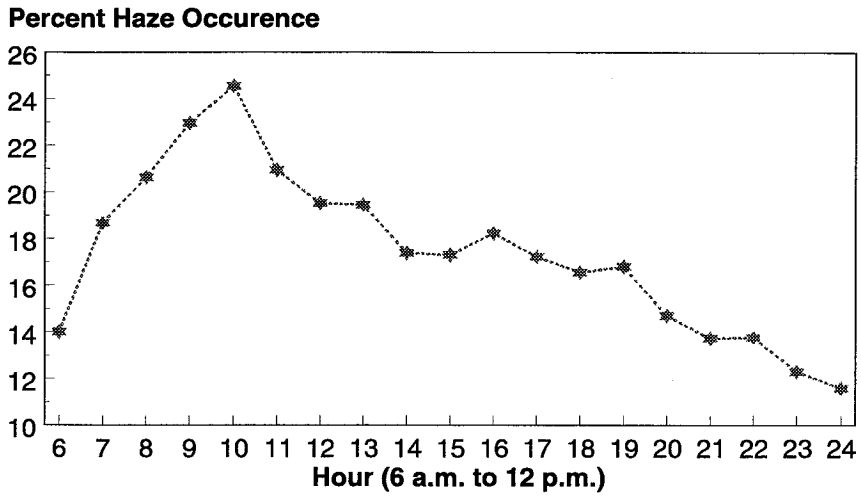

Although low ceiling and visibility are somewhat more common at DTW than BOS, average delays are less, even during IFR. Figure 2-11 shows average arrival delay during IFR1 of about 13 minutes, versus an average of over 40 minutes at BOS. When examining specific days of poor weather at the two airports, BOS shows many more very bad days when delays of a half hour to hour are routine. Such days are generally uncommon at DTW, as the parallel runways do not lose independent operations under IFR conditions. At BOS, IFR conditions result in single runway operations and their associated large flight capacity reductions.

Figure 2-11. Average Delays by Operating Conditions, DTW Arrivals in 1993

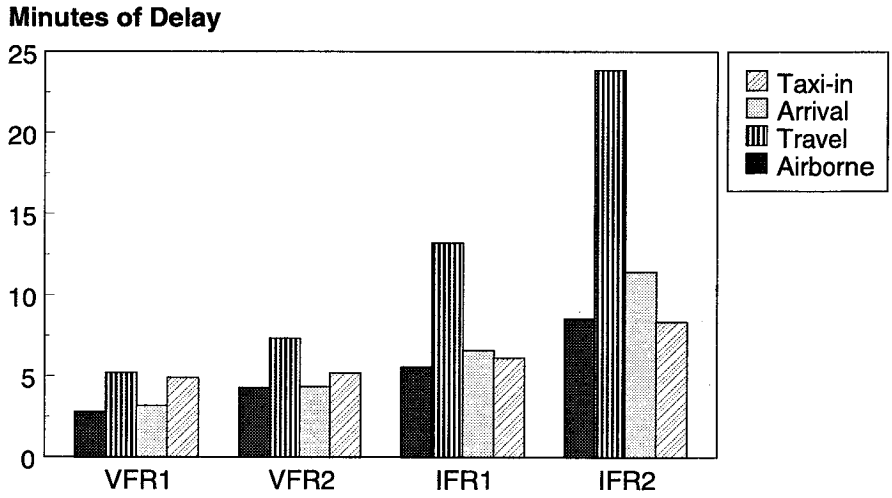

Figure 2-12. Delays by Phase of Flight and Time of Day DTW VFR1 Arrivals in 1993

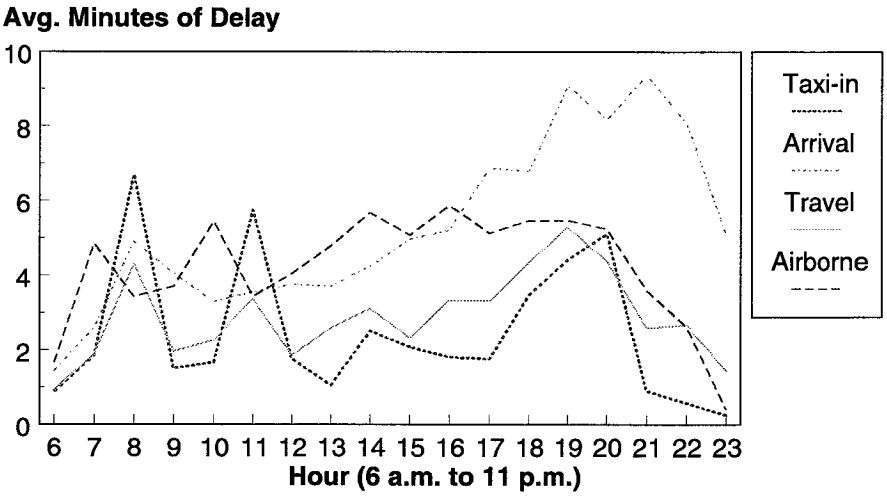

SUMMARY AND CONCLUSIONS ON OBSERVED DELAYS

We summarize our preliminary analyses in these terms:

- For all airport and month combinations considered, the days with the worst arrival delay performance were always associated with IMC. Instances in which weather-reduced capacity produced delay were identifiable in all airport and month combinations.
- For all airport and month combinations considered, days with the best arrival delay performance were always associated with VFR1.
- In most cases, interactions among weather, capacity, demand, and delay can be followed in detail.
- Different phenomena appear to be most significant for delays at the two airports studied; the degree to which meteorological conditions are associated with delay varies from airport to airport.
- Arrivals that occur in IMC account for significant fractions of total arrival delay. The fraction of arrivals that occur in IMC varies significantly from airport to airport.

We conclude the following:

- There are enough identifiable arrival capacity-reduction mechanisms to make possible an effective analysis of the specific effects of the TAP technologies.
- Identifiable arrival capacity-reduction mechanisms differ from airport to airport and enable the effective study of benefits of all three TAP technology groups.
- Even though IMC prevails only about 10 percent of the time overall, a significant fraction of delay is associated with IFR arrivals at many, if not most, airports.

Chapter 3
Modeling Airport Capacity

OVERVIEW

One of the key objectives of this analysis is to use an appropriate model to estimate the capacity of an airport as a function of weather, FAA procedures, and the level of technology available. We define airport capacity as a Pareto frontier of arrivals per hour, versus departures per hour. This frontier is the boundary of the set of points at which arrival rate and departure rate can be simultaneously increased.

Figure 3-1 gives an example capacity curve, taken from data prepared for an FAA study. The figure indicates that, when departures are given priority, Newark International Airport can accommodate up to 57 departures per hour. Up to 46 arrivals per hour can be integrated into the departure stream while maintaining that departure rate. Increasing the arrival rate above 46 per hour can only be done by decreasing the departure rate, up to an arrival rate of 50 per hour. This is the airport maximum arrival rate: Up to 48 departures per hour can be accommodated while maintaining that rate. (An airport capacity curve is not necessarily made up of straight-line segments like the example.)

Figure 3-1. Example Airport Capacity

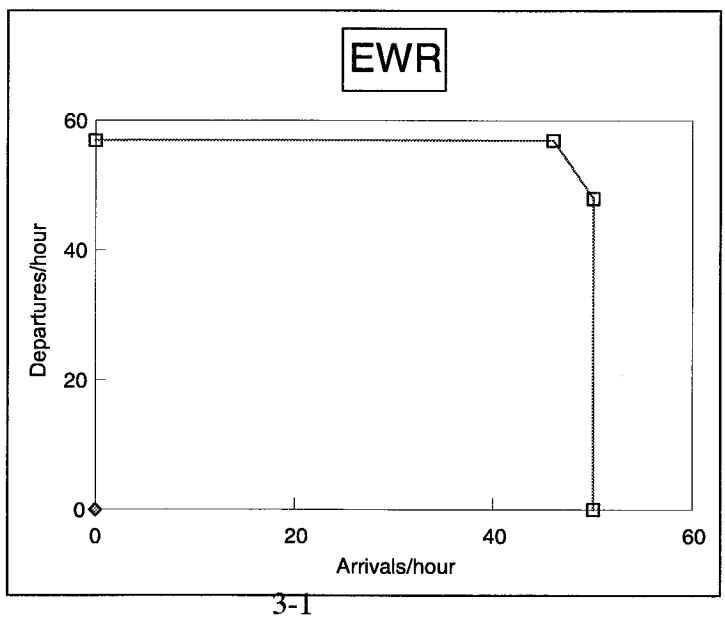

Actual airport capacity varies with, among other factors, ceiling, visibility, wind speed and direction, and the kinds of aircraft using the facility so that a complete specification of airport capacity is a family of curves like that of Figure 3-1.

This study requires the development of estimates of airport capacity, such as that shown in Figure 3-1, and their modification to reflect the impacts of the TAP systems. To do so, it is necessary to use an appropriate model that can estimate capacity as a function of weather conditions and those capacity parameters affected by the TAP systems. The resulting capacity estimates can then be used to calculate the reduction in delay for a given level of demand.

PARAMETRIC CAPACITY ANALYSES AND SIMULATIONS

Several models of airport capacity have been developed over the past three decades. These can generally be classified into two categories, simulations and analytical models. The simulation approach uses a highly detailed representation of airport and aircraft operations and extensive Monte Carlo iterations are required to analyze the impact of changes in runways, taxiways, procedures, and technological capability on airport capacity and delay. These simulations are usually required when evaluating changes to the physical layout of an airport or adjustments to its airspace. They require a great deal of data to operate, thereby requiring several months to complete a study of a single airport.

Analytical models use a limited set of parameters and produce results with a single execution. Analytical models are also used to estimate the impact of changes in procedures and technology on airport capacity. Because they do not require a highly detailed description of all aspects of airport operations or multiple runs, analyses of a single airport can often be completed in much less time than a simulation would require but with similar confidence in the results. The challenge in using an analytical airport model is specifying the parameters that reflect the impact of the procedures or technologies to be evaluated. The parameters commonly used for airport capacity analysis are miles in trail separations, arrival and departure runway occupancy times, the standard deviation of interarrival times (IATs), and aircraft mix. To the extent that parameters such as these can accurately reflect the effects of the TAP systems, an analytical model is ideal for the benefits analysis of this study. Analytical models do not, however, provide reliable insight into complex issues related to ground movement or detailed airspace operations. The most commonly used analytical model is the FAA Airfield Capacity Model; we performed an extensive evaluation of it for this study.

The approach used in the FAA Airfield Capacity model satisfies some, but not all, of the analytical requirements for this study. Most importantly, the model does not provide adequate mechanisms for incorporating the several effects of the TAP systems. For example, many of the TAP technologies provide advanced automation tools to pilots and controllers that will enable them to decrease the separation and improve the predictability of the spacing between arriving aircraft. In modeling terms, this automation reduces the variation in IAT. The FAA Airfield Capacity model enables users to input a standard deviation of IAT. But, to evaluate the TAP systems analysis, we need a model that derives the distribution of IAT in a rigorous fashion. Other TAP automation improves the quality of information available to controllers and speeds communications. Neither of these effects can be incorporated cleanly into the FAA model.

To overcome these deficiencies, LMI developed a new analytical model of runway and airport capacity that incorporates parameters related to the TAP systems. The LMI runway capacity model takes an air traffic controller-based view of airport operations. The limitations on the quality of information accessible to the controller—such as aircraft position and speed—directly affect the spacing required for safe operation of aircraft streams. Similarly, delays in communications affect spacing requirements through the need to provide sufficient time for the controller to provide instructions to aircraft.

Table 3-1 lists the key parameters used in the LMI Runway Capacity Model and the FAA Airfield Capacity Model. The important differences in the lists are those that affect the distribution of IAT. The LMI model estimates the distribution of IAT from the aircraft mix, the standard deviation in approach speed, the standard deviation in wind speed, and the standard deviation in position uncertainty. In the FAA model, the user simply inputs a value for the standard deviation of IAT. The different approach used by the two models is important for analyzing TAP since some of the crucial TAP systems, such as CTAS-FMS integration coupled with DGPS, will improve the quality of information available to the controller and, hence, reduce some of those uncertainties. The precise impact of those reduced uncertainties requires a rigorous analysis to determine their potential effect on the distribution of IAT. Appendix A describes the derivation of the LMI runway capacity model in greater detail and provides the Pascal code used to execute it.

Table 3-1. Capacity Model Parameters—Comparison

LMI-Runway Capability Model	FAA-Airfield Capability Model
p_i, fraction of aircraft in class I	p_i, fraction of aircraft in class I
S_{ij}, miles-in-trail minima	S_{ij}, miles-in-trail minima
Vi, approach speeds	V_i, approach speeds
D, common path length	D, common path length
R_{ai}, arrival ROT	R_{ai}, arrival ROT
σ_{Ai}, s.d. of arrival ROT	σ_{Ai}, s.d. of arrival ROT
R_{di}, departure ROT	R_{di}, departure ROT
σ_{Di}, s.d. of departure ROT	σ_{Di}, s.d. of departure ROT
D_d, distance-to-turn on departure	T_D, departure time interval σ_D, s.d. of departure time interval
V_{di}, departure speed	
σ_{Di}, s.d. of departure speed	σ_{TA}, s.d. of interarrival time
σ_x, s.d. of position uncertainty	
σ_{Vi}, s.d. of approach speed	
σ_w, s.d. of wind speed	
c, mean communications delay	c, mean communications delay
σ_c, s.d. of communications delay	

Note: Subscripts indicate variation with aircraft class. ROT = runway occupancy time; s.d = standard deviation.

Figure 3-2 shows an example of the runway capacity model output. The chart depicts a baseline arrival-departure capacity based on current arrival separation requirements. The outer capacity line reflects the impact of reducing those separations for all aircraft classes. While the chart is only illustrative, it does show the important features of the model:

- the tradeoff between arrivals and departures;
- direct treatment of the key TAP systems; and
- other effects, such as communications delay and aircraft mix.

Figure 3-2. Runway Capacity Model Output

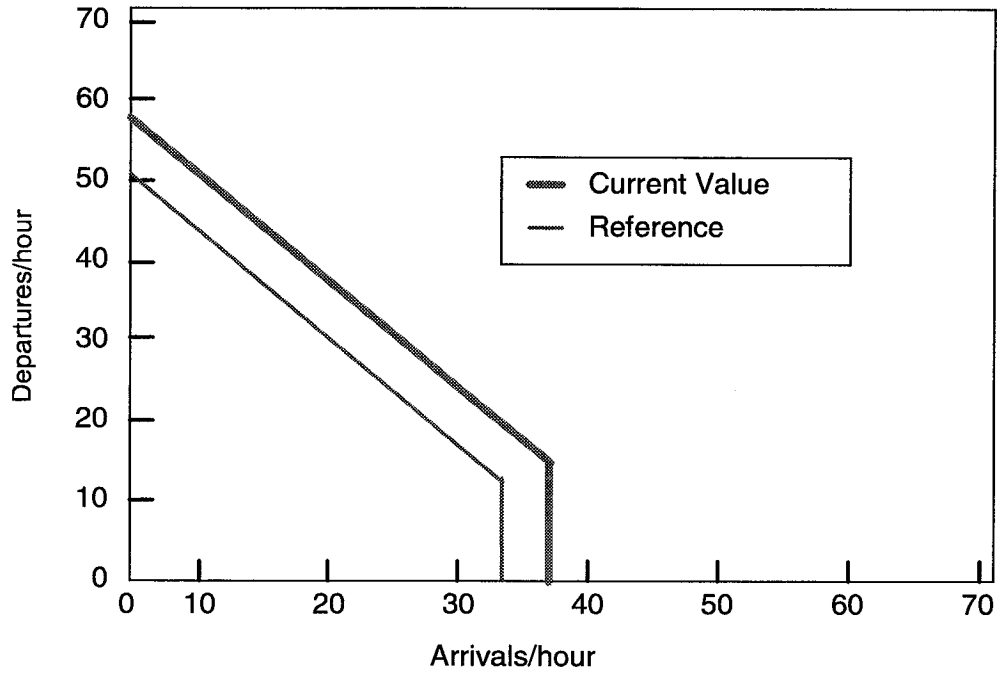

The two study airports do not usually operate with only one active runway during busy periods. Accordingly, for most conditions the capacity of an airport must be estimated by combining estimates of single-runway capacities into estimates for the capacities of combinations of runways operated simultaneously.

It is possible to estimate capacities of combinations of runways analytically. The task is trivial in some cases, such as when two runways are sufficiently separated that FAA regulations permit them to be operated simultaneously and independently. Parallel runways separated by more than 4,300 feet usually meet that condition. In more complex cases, analytic models may be developed by modeling the effects of FAA procedures governing dependent runway operations.

The actual operation of runway configurations at large airports often involves a good deal of airport-specific practice. For example, when DTW is operating in the 21L/21C/21R configuration, runway 21L is used for arrivals only, 21R is used for a mix of arrivals and departures that depends on demand, and runway 21C is used for departures only. Figure 3-3 shows the runway layouts at DTW, along with information on runway length and separations. Figure 3-4 provides similar information for BOS.

Since in this study we estimate the capacities of a relatively limited set of airports. It is both more efficient and more accurate to develop models of the specific runway configurations actually used at these airports, in consultation with the controllers who operate them, rather than to develop general multi-runway models and particularize them to a given airport. The airport capacity models used for this study were built that way.

The models generate estimates of airport capacity hour-by-hour based on the weather conditions in effect on the airport surface during that time, and the level of technology as reflected in the runway capacity model parameters. The sequence operates as follows:

1. estimate runway capacity as a function of available technology;

2. estimate the capacity of the airport runway configurations based on current weather and available technology;

3. determine the most effective runway configuration to use, based on estimated capacity and weather conditions;

4. generate an hourly series of airport capacities.

5. Appendix B provides more detailed information on the airport capacity models for BOS and DTW.

Figure 3-3. Detroit Figure from ASC Plan

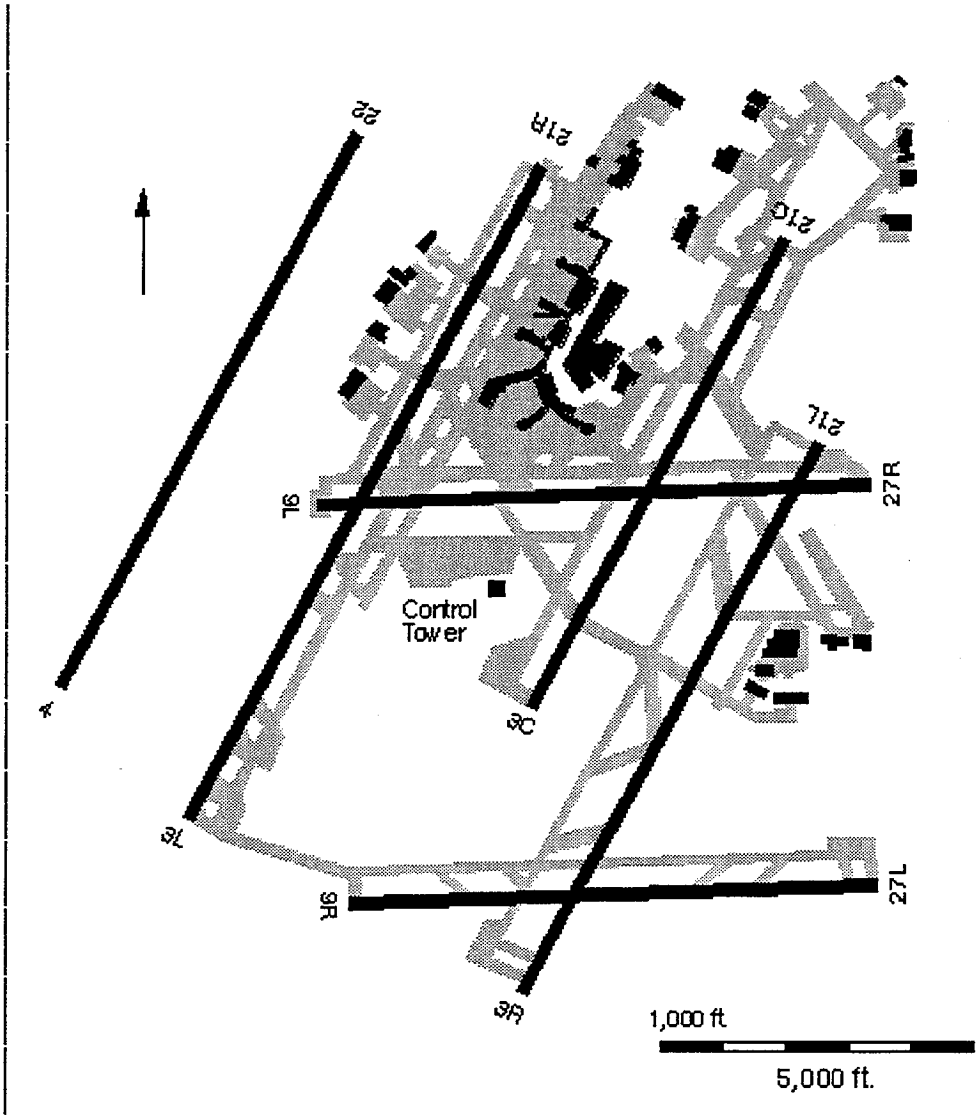

Latitude 42.22° N **Longitude** 83.35° W Great Lakes Region

Figure 3-4. BOS Airport Layout from ASC Plan

Figure 3-4. BOS Airport Layout from ASC Plan

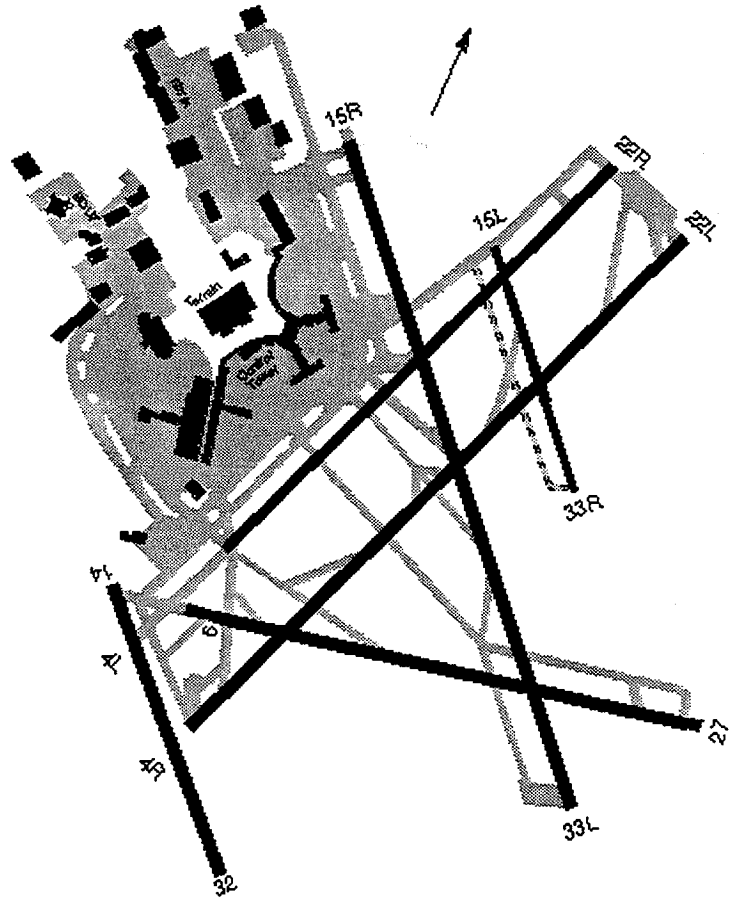

Latitude 42.37° N **Longitude** 71.0° W New England Region

Chapter 4
Estimating Delay

The runway and airport capacity models described in Chapter 3 satisfy the analytical requirement to estimate airport arrival and departure capacity as functions of weather and available technology. The next step is to estimate aircraft delays given airport capacity and demand. Queuing models are used for this. Comparing the resulting delays with and without the TAP systems gives estimates of TAP's impacts on delay.

QUEUING MODELS OF AIRPORT OPERATIONS

Many models of airports as queues are available. Malone[1] describes the considerations affecting their design and cites several examples. Queues are usually defined by specifying three features: the demand process, the service process, and the number of servers. (Sometimes a fourth feature, the maximum number of members that the queue may have, is added.)

The symbol "M" designates a Markov demand or service process, for which interarrival times or service times have a Poisson distribution.[2] Thus a queue described as "M/M/1" has Markov demand and service processes and one server. M/M/1 queues are widely used to model airport arrival and departure operations.

M/D/1 is another queue model used in airport analyses. The "D" indicates deterministic service (i.e., all service times are equal to a given constant). M/M/1 queues tend to overestimate airport delays, and M/D/1 queues tend to underestimate them. The queue model designated $M/E_k/1$, where E_k indicates that the service times have the Erlang-k distribution[3] with parameter k, gives delays between the M/M/1 and M/D/1 results.

---

[1] Malone, K. M., "Dynamic Queuing Systems: Behavior and Approximations for Individual Queues and for Networks," Section 1.2 and its references. Ph. D. dissertation, Sloan School of Management, Massachusetts Institute of Technology, June 1995

[2] The Poisson distribution is $p(t) = \lambda e^{-\lambda t}$

[3] The Erlang-k distribution is $p(t) = \frac{(k\lambda)\ t^{k-1}}{(k-1)!} e^{-k\lambda t}$

M/M/1, M/D/1, and M/E_k/1 all have relatively simple steady-state behavior when capacity exceeds demand. Unfortunately, these are not particularly helpful for airport studies because capacity is less than demand for many interesting cases—and also because, as pointed out by Odoni and Roth,[4] during busy periods airports rarely operate under fixed conditions long enough to reach the steady state.

In principle, exact unsteady results for M/M/1, M/D/1, and M/Ek/1 queues can be evaluated numerically. This may, however, require unacceptably long computing times. That motivates searches for approximations that give useful results in reasonable times. We have found one such approximation, the fluid model, particularly useful. It is described in the following section.

THE FLUID APPROXIMATION MODEL

The fluid approximation for a single queue of length q, with mean input rate λ and mean service rate μ, is the solution of the equation

$$\dot{q} = \begin{Bmatrix} \lambda - \mu, q > 0 \\ (\lambda - \mu)^+, else \end{Bmatrix}$$

where

$$(x-m)^+ \equiv \begin{Bmatrix} (x-m), (x-m) > 0 \\ 0, else \end{Bmatrix}$$

which takes on the value of the mean queue length at the initial time.

If λ and μ are piecewise constant functions of time, then the fluid approximation for q is a piecewise linear continuous function (i.e., a spline of order two (possibly on a knot sequence that is a refinement of the knot sequence for λ and μ[5]). This fact allows simple numerical schemes to generate fluid approximations rapidly—this is the fluid approximation's great advantage. The sense in which the fluid approximation for queues and queuing networks is a rational asymptotic expansion is discussed by Mandelbaum and Massey[6] and by Chen and Mandelbaum.[7]

---

[4] Odoni, A. R., and E. Roth, "An Empirical Investigation of the Transient Behavior of Stationary Queuing Systems," *Operations Research* 31, pp. 432-455, 1983.

[5] The "knot sequence" of a spline is the set of points at which the function's defining parameters may change.

[6] Mandelbaum, A., and W. Massey, "Strong Approximations for Time-Dependent Queues," *Mathematics of Operations Research* 20, pp. 33-64, February 1995.

The fluid approximation generally gives useful approximations for airport delays that are associated with utilization ratios, $\rho \equiv \lambda / \mu$, that are significantly greater than one for extended periods. Boston's Logan International Airport appears to be one at which such delays account for the bulk of total delays. Figure 4-1 compares the exact mean queue for a M/M/1 model of a reduced capacity period at BOS, with the fluid approximation for the same period. The results show the approximation to be excellent, with a relatively constant difference that is readily calculated.

Figure 4-1. Exact Mean Queue and Fluid Approximation

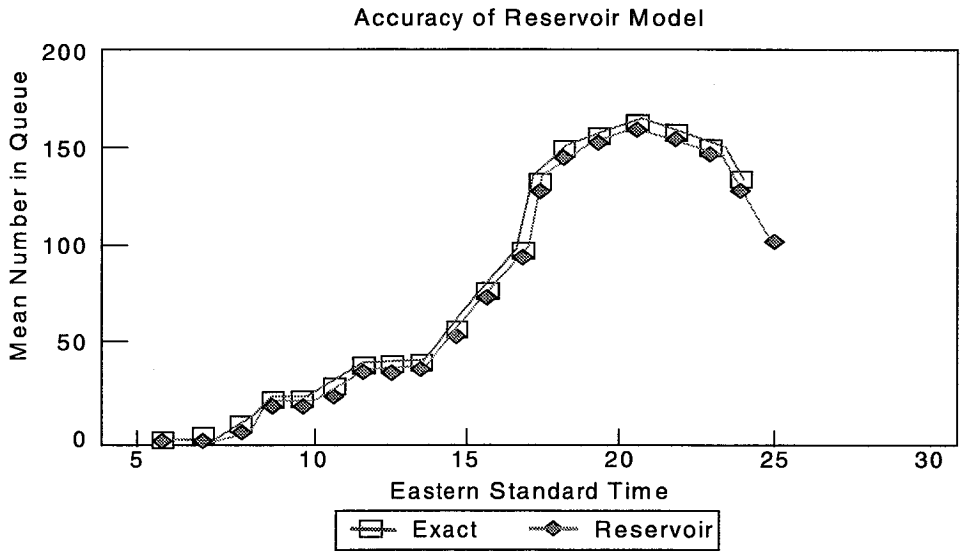

It is important not to use the fluid model when the utilization ratio, λ/μ, stays less than one, but very close to one, for extensive periods. In these cases, while the fluid model gives zero queue size, the actual queue may become significantly large. The analysis used in this study tests for these cases, and uses numerical integration to determine queue properties when they occur.

Modeling Arrival and Departure Demand

The previous chapter described how capacity can be estimated as a function of weather and available technology. Airport operations demand is also a key part of

[7] Chen, H., and A. Mandelbaum, "Discrete Flow Networks: Bottleneck Analysis and Fluid Approximations," *Mathematics of Operations Research* 16, pp. 408-446, 1991.

that analysis. For this study, we use hourly tower counts of arrivals and departures during representative days as the measure of demand placed on the airport. Since actual operations on days with reduced capacity are significantly affected by the poor weather, we use the arrival and departure counts on VMC days with no delay as the baseline demand for estimating delays on IMC days. That is, arrival delays on IMC days are based on the assumed desired mix of arrivals and departures that is typically found on VMC days.

The available demand data for BOS are the tower records of arrival and departures for May 20, 1993 through February 5, 1995. Through a statistical analysis of the records, we identified six distinct demand patterns. These six patterns are: winter weekdays, winter Saturdays, winter Sundays, summer weekdays, summer Saturdays, and summer Sundays. These days represent the regular weekly and seasonal variations in demand at BOS.

The demand data available for analyzing DTW are processed from ARTS tapes for the week of July 16-22, 1995. Since the FAA controllers at DTW reported that demand does not vary much with the seasons at DTW, three representative days were used to analyze DTW. These days are Saturday, Sunday, and Thursday in the week of July 16-22, 1995.

These demand counts and patterns serve as the principal driving force for estimating delays in this study. This approach differs from the methods typically used in other studies, which usually measure delay as the difference between actual arrival time and some scheduled time, such as from the OAG or a flight plan. The approach developed in this study has two advantages: First, it directly estimates the delay attributable to IMC conditions, without reference to any possible "schedule padding" used by the airlines. Second, the use of hourly counts reduces the computational burden considerably. Although some precision is lost by ignoring scheduling peaks within each hour, this method preserves the overall estimate of delay reduction that is needed to provide preliminary estimates of the benefits from the TAP program. Our interest is not so much in the delay experienced by a specific flight as it is in the overall reduction in delay experienced by all flights arriving at an airport.

Chapter 5
Estimating the Impacts of TAP Technologies on Capacity and Delay at BOS and DTW

This chapter shows how we applied the methods described above to analyze the effects of implementing TAP technologies at BOS and DTW. The approach unfolds in six steps:

1. Select the model parameters that accurately reflect the technology states.
2. Calculate airport capacity as a function of weather and the level of available technology.
3. Estimate the delay reduction from TAP for specific days and demand patterns.
4. Devise a method to annualize the delay estimates.
5. Devise a method to estimate delays through the year 2015, with and without the TAP systems.
6. Translate the delay reductions due to TAP into airline operating cost savings.

The remainder of this chapter describes the first five steps listed and Chapter 6 addresses the methods for translating delay reductions into airline cost savings.

Capacity Model Parameters and Their Correlation with TAP Technologies

In modeling airport capacity, we relied primarily on the LMI models described in Chapters 3 and 4 . We did so because it is simpler to relate the TAP systems effects to parameters of the LMI model than to parameters of the FAA capacity model and because documentation of the FAA model does not describe some important features in adequate detail. We did carry out a parallel modeling effort based on the FAA model to provide a comparison.

In this chapter, we describe the input parameters of the LMI capacity models and how they are affected by TAP technologies. We first describe the five technology states considered. Following that, we address the model parameters, how they relate to the TAP technologies, and what values are appropriate for each technology state.

THE FIVE TECHNOLOGY STATES MODELED

The five technology states modeled are a current reference consisting of the IFR conditions that exist today; a 2005 baseline, and three increments of TAP technology.

Current Reference. The model parameters for the Current Reference were obtained largely from FAA-EM-78-8A, *Parameters of Future ATC Systems Relating to Capacity/Delay*, June 1978, and the *Upgraded FAA Airfield Capacity Model, Volume 1* (hereafter referred to as "the User's Guide"), May 1981. These were supplemented by information from NASA and FAA personnel and with information from the *Air Traffic Control Handbook*, FAA 7110.65. The Current Reference uses the aircraft classifications and wake vortex separations defined in FAA Safety Notice N 7110.157, July 16, 1996.

2005 Baseline. We assumed that the TAP systems would not be fielded and operational until the year 2005, so that year was used as the baseline. Between now and 2005, several enhancements to existing capabilities that are not part of TAP are expected to become available for general use. The 2005 baseline assumes deployment of the Center/TRACON Automation System (CTAS) and the implementation of the Wide Area Augmentation System (WAAS). All aircraft are assumed to be equipped with Global Navigation Satellite System (GNSS) equipment. The impact of these technologies includes reduction in aircraft position uncertainties and a modest expansion of approach path alternatives.

TAP 1. The first TAP increment includes the Aircraft Vortex Spacing System (AVOSS) with wake vortex sensors and upgraded TCAS information on lateral spacing. We expect these elements, along with CTAS/GPS, to enable reduced separations for traffic behind B757 and heavy aircraft.

TAP 2. The second TAP increment includes the TAP 1 systems and adds technologies being developed in the Low Visibility Landing and Surface Operations (LVLASO) program. LVLASO programs include the Dynamic Runway Occupancy Measurement system (DROM), the Aircraft Rollout and Turnoff (ROTO) system, and the Aircraft Taxi-Navigation and Situational Awareness (T-NASA) system. Specific technical capabilities include GPS precision landing capability plus any cockpit taxi maps and sensor systems necessary to reduce arrival runway occupancy time (ROT).

TAP 3. The third TAP increment includes TAP 1 and TAP 2, plus integrated CTAS/FMS. Integration assumes two-way CTAS/FMS data linking. In the TAP 3 increment, CTAS would be operating "closed loop" with the current flight plans of individual aircraft based on data from the FMS. Moreover, the FMS will provide high confidence that the plans will be carried out as described. Flight plan revisions will be communicated both ways in real time. The precise knowledge of the relative positions of all traffic will enable execution of specific "soda straw" flight paths to avoid wake vortices. The parametric result will be reduced uncertainty about aircraft status and intent that can be used to safely reduce IFR separations to VFR distances.

We discuss specific modeling parameters and the values they assume in the five technology states in the following subsections.

Model Parameters and Their Relations to the Technology States

Table 5-1 lists the parameters used in the LMI runway capacity model. For comparison, it also shows the parameters used in the FAA Airfield Capacity Model.

Table 5-1. Runway Capacity Model Parameters; Comparison

LMI-Runway Capacity Model	FAA-Airfield Capacity Model
p_i, fraction of aircraft in class i	p_i, fraction of aircraft in class i
S_{ij}, miles-in-trail minima	S_{ij}, miles-in-trail minima
V_i, approach speeds	V_i, approach speeds
D, common path length	D, common path length
R_{Ai}, arrival ROT	R_{Ai}, arrival ROT
σ_{Ai}, s.d. of arrival ROT	σ_{Ai}, s.d. of arrival ROT
R_{Di}, departure ROT	R_{Di}, departure ROT
σ_{Di}, s.d. of departure ROT	σ_{Di}, s.d. of departure ROT
D_d, distance-to-turn on departure	T_D, departure time interval σ_D, s.d. of departure time interval
V_{Di}, departure speed	
σ_{Di}, s.d. of departure speed	σ_{TA}, s.d. of interarrival time
σ_x, s.d. of position uncertainty	
σ_{Vi}, s.d. of approach speed	
σ_w, s.d. of wind speed	
c, mean communications delay	c, mean communications delay
σ_c, s.d. of communications delay	

Note: *Subscripts indicate variation with aircraft class. ROT = runway occupancy time; s.d. = standard deviation*

Runway Configuration

As detailed in Chapter 3, the Airport Capacity Model estimates arrival and departure capacity combining outputs from the LMI Runway Capacity Model according to operating rules provided by controllers at the subject airports. Estimating airport capacities requires constrained super position of runway model results. The constraints generally reflect air traffic control (ATC) operating procedures with items like time delays for clearing intersections and distance minimums for interleaved departures and arrivals. The airport models check interarrival times, runway clearing times, plus any additional constraint conditions, to insert departures between arrivals. Departures are estimated in the same manner.

For each of the airports studied, the same runway configurations are used for the Current Reference, 2005 baseline, and the TAP increments. We assume that GPS and TAP technologies (particularly information for lateral spacing) will allow independent use of parallel runways spaced greater than 2,500 feet apart. As it happens, neither of the two airports studied has runways in this class that are not also sufficiently widely spaced for independent operation under present rules (i.e., ≥4,300 feet).

AIRCRAFT MIX

We currently model four classes of aircraft in the operational mix. The small, large, and heavy categories are classed by takeoff gross weight (TOGW) as shown in Table 5-2. In addition to these standard categories, the Boeing 757 is added as a fourth aircraft class, between the large and heavy categories.

Table 5-2. Aircraft Weight Categories

Category	Take-off Gross Weight
Small	TOGW < 41,000
Large	41,000 < TOGW < 300,000
Heavy	TOGW > 300,000

Average Official Airline Guide (OAG) data for 1993 provided the percentages of operations in each aircraft class. While the OAG does not include all flights (it excludes private, military, and some airfreight), we assumed that the ratios were reasonable for the purpose of analysis. In the case of Boston, we acquired tower data that provided a more complete and accurate history of operations. The aircraft ratios derived from the Boston tower data did not differ significantly from those derived from the OAG data.

ARRIVAL RUNWAY OCCUPANCY TIMES

Arrival runway occupancy times (ROTs) are required for each arrival runway modeled. Sufficient field data are not available for all configurations and conditions to be modeled, so analytic techniques are necessary to provide the required model input.

Current Reference. We produced the Current Reference arrival ROTs using the analytic method and values contained in *the User's Guide for the FAA Airfield Capacity Model.* We checked the results with ROT data when possible.

For dry normal, dry high-speed, and wet runway exits the *User's Guide* provides tables of exit ROT versus distance from runway threshold and cumulative probability of exit use versus distance from runway threshold for each of four classes of aircraft (i.e., small, small jet, large, heavy). Total runway ROT for a given class of aircraft is determined by establishing the exit distances for the runway, entering the ROT/distance table to determine exit ROT, entering the probability/distance table to determine probability of exit use factor, multiplying the ROTs by the probability factors, and finally adding up the results. In our analyses, we determined the exit distances from the airport diagrams contained in the U. S. Terminal Procedures "approach plates."[8]

The *User's Guide* tables are constructed for distances that are integral multiples of 1,000 feet. In order to enter other values and automate the ROT calculations, we generated curve fits to the table values and incorporated them into a short computer program. This program speeds the analysis process and also enables direct comparison of field data with the *User's Guide* model.

Unfortunately, the agreement between the ROT tables and collected data is often poor. The differences that exist are generally within one standard deviation of the data sample means, but the data are scattered and the standard deviations are large. The table values for dry runways consistently agreed better with the measured data than the table values for wet runways. Several researchers, supported by the sparse historical data taken under IMC conditions, report that there is little or no difference between VMC and IMC ROTs. Consequently, the dry runway values from the model are used in all cases.

The standard deviation of arrival ROT is an input parameter for the capacity models. The standard deviation parameter covers both the variations in pilot performance for given exits and the variations in exit selection by the pilots. The pilot performance

[8] *U. S. Government Flight Information Publication, U. S. Terminal Procedures*, Department of Commerce.

uncertainty corresponds to uncertainty in the ROT versus distance tables in the *User's Guide*. The exit choice uncertainty corresponds to uncertainty in the probability use versus distance tables in the *User's Guide*. TAP technologies may lead to improvements in the pilot performance uncertainties, but exit use is dependent on many external issues such as gate location, dynamic taxiway congestion, and construction that are not addressed by TAP.

Eight seconds is the value of arrival ROT standard deviation used for the Current Reference based on FAA-EM-78-8A. Eight seconds is on the low end of available field data, but there is no compelling logic to justify selection of a higher value.

2005 Baseline. We do not expect arrival runway occupancy times or their uncertainties to change in the 2005 baseline.

TAP 1. The TAP 1 technologies will not affect runway occupancy times.

TAP 2. The TAP 2 environment includes wide deployment of integrated GNSS/roll-out and turn-off (GNSS/ROTO) capability plus electronic taxi maps. These technologies are modeled by reducing arrival ROT by 20 percent for each class of aircraft. [9]

The ROT uncertainty may be reduced due to improved landing precision, but the model parameter was not changed because (1) it is difficult to separate pilotage uncertainties that may be reduced from exit selection uncertainties that are unaffected, and (2) the base value of ROT uncertainty is already on the low end of the data.

TAP 3. No further reductions in ROT beyond TAP 2 are assumed for TAP 3.

IFR Minimum Interarrival Separations

The minimum interarrival separations are strong drivers of airfield capacity both in the models and in the real world. The IFR baseline values we use are those contained in the *Air Traffic Control Handbook*, FAA 7110.65H. The IFR separations recently were modified by FAA N 7110.157 to require a 5 nautical mile (nmi.) separation for small aircraft following Boeing 757s. The VFR separations are taken from FAA-EM-78-8A and are reputedly based on unidentified "field data." FAA-EM-78-8A is old, but no major change in either operations or modeling has occurred since it was published. In addition, we find that the FAA-EM-78-8A values are still commonly used in analyses, and we have no data to justify using others. Interarrival separations are divided by aircraft speed to produce minimum interarrival times.

[9] Twenty percent ROT reduction (50 seconds to 40 seconds) is the LVLASO goal stated in the draft *Level III* plan.

There are two distinct reasons for FAA separations. The first is the requirement for controllers to safely manage aircraft given the available displays, communications, and data rates. This requirement is the reason for the fundamental 3.0 nmi. minimum separation. The second reason for separation is wake vortex hazard. Wake vortex hazard is the cause of all separations greater than 3.0 nmi.

Current Reference. The current reference IMC minimum interarrival separations are given in Table 5-3. FAA 7110.65 allows 2.5 nmi. separations in place of the 3.0 nmi. minimums under conditions that include documented ROTs under 50 seconds. One runway at Detroit and all runways at Boston meet the requirements under dry conditions. Both airports revert to 3.0 nmi. minimums when the runways are wet. Since runways are normally wet during IMC conditions we use 3.0 nmi. minimum separations during IFR. We use the 2.5 nmi. minimum for VMC 2 conditions when radar control is required, but the runways are usually dry.

Table 5-3. Current Reference Interarrival Separations (in Nautical Miles)

	Trail			
Lead	Small	Large	B-757	Heavy
Small	3.0	3.0	3.0	3.0
Large	4.0	3.0	3.0	3.0
B-757	5.0	4.0	4.0	4.0
Heavy	6.0	5.0	5.0	4.0

2005 Baseline. CTAS and universal GNSS will not change the minimum separations.

TAP 1. The TAP 1 interarrival separation minimums are given in Table 5-4. The wake vortex prediction/detection capability introduced in TAP 1 will enable moderate reductions in the separations behind large and heavy aircraft, but will not enable reductions below the 3.0 nmi. minimum.

TAP 2. The TAP 2 LVLASO technologies result in ROTs less than 50 seconds under all meteorological conditions and, thus, allow use of 2.5 nmi. minimum separations in place of the 3.0 nmi. separations in Table 5-4.

Table 5-4. TAP 1 Interarrival Separations (in Nautical Miles)

Lead	Trail			
	Small	Large	B-757	Heavy
Small	3.0	3.0	3.0	3.0
Large	3.5	3.0	3.0	3.0
B-757	4.0	3.5	3.5	3.5
Heavy	5.5	4.5	4.5	3.5

TAP 3. The TAP 3 implementation includes CTAS/FMS integration plus reliable situation awareness Airborne Information for Lateral Spacing (AILS) that will enable operation with the VFR (FAA-EM-78-8A) separations given in Table 5-5. We note that significant changes in the roles of air controllers, pilots, and automation must be resolved before TAP 3 separations can be achieved.

Table 5-5. TAP 3 Interarrival Separations (in Nautical Miles)

Lead	Trail			
	Small	Large	B-757	Heavy
Small	1.9	1.9	1.9	1.9
Large	2.7	1.9	1.9	1.9
B-757	3.5	3.0	3.0	2.7
Heavy	4.5	3.6	3.6	2.7

INTERARRIVAL TIME UNCERTAINTY

The interarrival time uncertainty, σ_{TA}, is an input parameter in the FAA model. The uncertainty is expressed as the standard deviation, in seconds, of the interarrival time. One value of σ_{TA} is used for all aircraft classes and leader/follower pairs. The uncertainty time is multiplied by a probability factor and added to the minimum interarrival time to produce a working time interval that has high confidence of not violating the

separation minimums. The normally used confidence is 95 percent with a corresponding factor of 1.65.

The LMI runway capacity model, as described in Chapter 3, has separate inputs for uncertainties in position, approach speed, and wind speed. The model applies these uncertainties to the specific aircraft leader/follower pairs as they fly the approach common path (common path is discussed below). The model applies confidence margins to the resulting uncertainties in interarrival time to ensure against violation of minimums.

The LMI model results make clear the fact that interarrival time uncertainties vary significantly with leader/follower characteristics and with common path length. A composite interarrival time uncertainty that corresponds to the FAA model σ_{TA} can be calculated as an output by the LMI model for comparison with the FAA model input.

Interarrival time "error" data are available from man-in-the-loop final approach spacing aids (FASA) simulations performed by NASA.[10] In the FASA experiments for CTAS supported cases, the difference between the minimum arrival time predicted by CTAS and the arrival time achieved by the controller was calculated for each flight. In cases not supported by CTAS, the difference between the minimum allowed separation and the actual threshold separation was calculated for each flight. The differences in the times for sequential flights were calculated and defined as the interarrival time errors. Means and standard deviations of the interarrival time errors were computed. With some caution, the standard deviations can be compared to σ_{TA}.

It must be kept in mind that the uncertainty values used in the models represent the controller's view. Improvements in the knowledge of position using GNSS, for example, will not result in reduced separations unless the information is communicated to the controller in a way he can use it (e.g., through CTAS to a final approach spacing aid).

Current Reference. The LMI values for the uncertainty parameters of approach speed, position, and wind were selected in the light of discussions with pilots and controllers. These parameters, along with the common path length and Boston aircraft mix, lead to a composite 17 second standard deviation of interarrival time. The FAA model current reference interarrival time uncertainty is 18 seconds (one standard deviation), taken from FAA-EM-78-8A. The values for all the parameters, plus the error data from the NASA simulation are shown in Table 5-6.

[10] *Final Approach Spacing Aids (FASA) Evaluation for Terminal-Area, Time-Based Air Traffic Control*, Credeur, et al, NASA Technical Paper 3399, Dec 1993.

Table 5-6. Interarrival Time Uncertainty Parameters

Parameter	Current	2005	TAP 1	TAP 2	TAP 3
LMI Model Approach Speed, σ_{Vi} (knots)	5	5	5	5	4
LMI Model Position, σ_X (distance)	0.25 (nmi.)	100 (feet)	100 (feet)	100 (feet)	100 (feet)
LMI Model Wind Speed, σ_W (knots)	7.5	7.5	7.5	7.5	5
LMI Composite Uncertainty (seconds)	17	13	13	13	10
FAA Model IAT Uncertainty, σ_{TA} (seconds)	18	12	12	12	8
NASA Interarrival Errors (seconds)	15.4-18.8	8.2-13.9	NA	NA	NA

2005 Baseline. In the LMI model, the 2005 baseline is modeled by reducing the position uncertainty, σ_x, to 100 feet, in view of the position accuracy afforded by GNSS and, as discussed below, reducing the common path length to 5 miles. These changes produce a composite standard deviation of interarrival time of 13 seconds. For inputs to the FAA model, we estimate that CTAS and universal GNSS will improve the position accuracy and correspondingly reduce the interarrival uncertainty from 18 to 12 seconds. The data from the NASA simulations gave a range of 8.2 to 13.9 seconds for interarrival errors when using CTAS and the best of the semiautomated spacing aids.

TAP 1. TAP 1 technologies are not expected to affect interarrival time uncertainties.

TAP 2. TAP 2 technologies are not expected to affect interarrival time uncertainties.

TAP 3. In the LMI model, TAP 3 technologies reduce wind speed standard deviation to 5 knots due to the ability of the integrated CTAS/FMS to plan optimized flight paths. The remaining uncertainty is due to individual pilot and airline preferences, which may not conform to the optimum path. In TAP 3, the FMS will also reduce the uncertainty in approach speed due to the more precise speed control by the FMS and the transmission of reliable intent information to the CTAS computer. In the FAA

model, the integration of ATC and FMS in TAP 3 is expected to reduce the interarrival time standard deviation to 8 seconds.

APPROACH SPEEDS

The values for approach speeds used in our analyses are slightly higher than those of the examples in the *User's Guide*. We based our approach speeds on discussions with airport controllers about the approach speeds they observe. The approach speeds do not change with time or TAP technology.

WIND SPEED STANDARD DEVIATION

Wind speed standard deviation is an input for the LMI model. This parameter reflects two effects. First, winds vary with time, so that leader and follower generally experience different winds. Second, winds aloft vary with altitude, and leader and follower may fly different approach profiles, which also causes the two aircraft to experience different winds.

DEPARTURE RUNWAY OCCUPANCY TIME

Departure ROTs are not addressed in FAA-EM-78-8A. The departure ROTs we used are based on the examples in the *User's Guide*. Departure ROTs are typically short and do not limit airport capacity. Departure ROTs are not affected by either CTAS/GNSS or the TAP technologies.

The uncertainty in departure ROT appears in both models. The current reference value of six seconds (one standard deviation) is used for all cases. Departure ROT uncertainty may be reduced by improved taxi precision, but no reductions were made in the model because there was no basis on which to predict or defend a specific value.

DEPARTURE SEPARATIONS

Departure time separations are specified in the FAA model and shown in Table 5-7. In the LMI model, departure miles-in-trail minima (currently assumed to be the same as arrival miles-in-trail minima) are imposed, as is a 60-second minimum time between departure clearances implied by FAA 7110.65H. Two switchable parameters are included in the LMI model. The first implements the FAA radar control practice for runways being used for both arrivals and departures of not releasing a departure if the next arrival is within 2.0 nmi.[11] This flag is set when meteorological conditions

[11] *Air Traffic Control*, FAA 7110.65H, paragraph 5-114, Note 1.

do not allow the controller to see the arrival at 2.0 nmi. from the threshold. The second parameter is a 2-minute hold for departing aircraft when the preceding departure is a heavy aircraft.[12]

Table 5-7. Current Reference Departure Separations in Seconds

Lead	Trail			
	Small	Large	B-757	Heavy
Small	60	60	60	60
Large	60	60	60	60
B-757	60	60	60	60
Heavy	120	120	60	60

Current Reference. The current reference values shown in Table 5-7. are taken directly from FAA 7110.65H restrictions.

2005 Baseline. The departure separation restrictions are not expected to change for the 2005 CTAS/GNSS baseline.

TAP 1. The departure separation restrictions are expected to be reduced by the TAP 1 AVOSS technology. In the TAP 1 case, for both the FAA and LMI models, all separations are expected to be 60 seconds based on the ability to confirm the absence of wake vortices.

TAP 2. TAP 2 technologies offer no further improvement in departure separations.

TAP 3. TAP 3 technologies enable removal of the departure hold requirement that is imposed when arrivals are within 2 nmi. of the threshold. The change is due to the controller's ability to accurately predict the movements of arriving aircraft regardless of meteorological conditions.

COMMON PATH LENGTH

The common path length is the distance from the threshold up the extended centerline within which the controller issues no further speed change directions. If a slower aircraft is following a faster aircraft the controller will establish the minimum spacing at the beginning of the common path. In the capacity models, the common path length

[12] *Air Traffic Control*, FAA 7110.65H, paragraph 3-155f.

is multiplied by the difference in aircraft speeds to determine the additional separation that occurs when a slower aircraft is following a faster aircraft. In the LMI model, the uncertainties in wind speed and approach speed are applied over the common path to calculate interarrival time uncertainty for all aircraft. Reductions in the common path reflect physical reductions in the common path due to curved/angled approaches.

Current Reference. An IFR common path length of 6 nmi. is used for all aircraft. This value is taken from both FAA-EM-78-8A and the *User's Guide*.

2005 Baseline. GNSS, like MLS, should allow curved and angled approaches with a reduced common path. While we do not believe large reductions will be made for many years, if ever, we do expect to see modest approach path optimizations with CTAS/GNSS operation. We assume these will result in a 1 nautical mile reduction in the common path (6 nmi. to 5 nmi.) due to modest adjustments to approach flight paths.

TAP 1. TAP 1 technologies will not further reduce the common path.

TAP 2. TAP 2 technologies will not further reduce the common path.

TAP 3. Integrated CTAS/FMS technologies will enable both extremely accurate prediction of aircraft performance and use of curved/angled approach paths, but these improvements are too uncertain to warrant further reductions in the common path at this time.

Crossing Runway Arrival/Departure Separation

This parameter is the amount of time the release of a departing aircraft is held up after an arriving aircraft has crossed the threshold of a crossing runway. We use 5 seconds for near-end crossing runways based on discussions with Boston controllers. We use 30 seconds for far-end crossing runways to ensure that the arriving aircraft are not going around, but this value has not been confirmed with controller personnel. The crossing runway separation parameter is not affected by CTAS/GNSS or TAP technologies.

Runway Model Results

Table 5-8 displays the LMI and FAA model results for a single runway during IMC. The runway modeled is Boston 4-Right, which is ILS-equipped. The good agreement with the FAA Capacity Model for the maximum arrival capacities and the affirmation of the results by Boston controllers as described in Appendix A give sufficient confidence in the LMI model to use it for the full airport capacity analysis. The disparity

between the LMI model and the FAA model for departures (and, consequently, 50:50 estimates) is not a major concern because the FAA model is known to overestimate departures.

Table 5-8. Comparison of LMI and FAA Capacity Model Results for a Single Runway at BOS

Operating Condition	Current Reference	2005 Baseline	TAP 1	TAP 2	TAP 3
Maximum Arrivals					
LMI (arrivals/departures)	32/8	34/5	36/2	39/4	52/17
FAA (arrivals/departures)	31/27	34/25	36/24	39/25	52/9
EPS (arrivals/departures)	28/8				
50:50 Operation					
LMI (arrivals/departures)	25/25	25/25	25/25	27/27	39/39
FAA (arrivals/departures)	30/30	31/31	31/31	33/33	35/35
EPS (arrivals/departures)	23/23				
Maximum Departures					
LMI (arrivals/departures)	0/43	0/43	0/44	0/48	0/55
FAA (arrivals/departures)	0/56	0/56	0/60	0/60	0/60
EPS (arrivals/departures)	10/40				

Note: The FAA Engineered Performance Standards (EPS) estimates are for a single runway, not specified.

TIME SERIES OF WEATHER AT BOS

We used the NCDC data to generate files of hourly data on ceiling, visibility, wind speed, wind direction, and temperature at BOS for 26 years: 1961 to 1964, and 1969 to 90. Records for 1965 to 1968 were omitted because the NCDC records for those years give data only every 3 hours.

For each year, we identified the days on which there was at least one hourly report of IMC conditions, in the hours 06:00 to 22:00 Eastern Standard Time. That is the period during which capacity reductions are most likely to cause significant delays. For each day thus identified, we extracted hourly data for 06:00 through 03:00 the following day. These 22-hour periods were adequate for queues to return to zero for most of the IMC days.

We analyzed the IMC day records in detail, using the modeling approach described in Chapters 3 and 4. While the IMC days account for most of the delay at BOS, there is some contribution from other days. To account for this, we identified a set of VMC days and computed the average delay for these days with the full M/M/1 model for

each year studied. Then we added the product of the number of days that were VMC and the average delay on VMC days, to the total delay for the bad days (estimated from the reservoir model). The VMC days corrections were small, usually around 15 percent of the total delay.

TIME SERIES OF WEATHER AT DTW

When we applied the procedure used at BOS to DTW, we found qualitatively different results that caused us to modify the approach. Both delay data and the models indicate that delays at BOS are largely due to bad days. Delays at DTW, however, are much less dominated by days with substantial periods in which capacities are significantly below demands. A much greater fraction of delays at DTW, approaching 50 percent, comes from days on which demand sometimes approaches capacity, but does not exceed it.

To cope with this different pattern, we treated DTW by considering all the days of the year, using as our inputs weather data from 06:00 Local Standard Time (LST) through 03:00 LST the following day. First, we generated the predictions of the reservoir model for all days of the year, for 06:00 LST to 03:00 LST the following day. Then we scanned all days for cases in which demand approached capacity from below. We computed delays for each such day by the full M/M/1 differential equations.

We also identified a set of four good days, one from each quarter of the year. We evaluated delays for these days with the M/M/1 equations, and used the average of these delays to represent delay on a good day.

We then accumulated delays for each day as follows: For a day on which demand approached capacity from below, we used the M/M/1 result. For all other days, we used the sum of the good-day delay and the reservoir model.

The reservoir model gives zero delay except when demand exceeds capacity. On days in which demand exceeds capacity for extended periods, the reservoir model predicts significant delays and, as is discussed in Chapter 4, is a good approximation to the full M/M/1 result. Thus, the sum of the reservoir model and the representative good-day delay is close to the good day figure, except when demand significantly exceeds capacity. For those days, the sum is close to the M/M/1 result.

FUTURE DEMAND AT BOS

The next step is to calculate a demand series for the years 2005 through 2015 when the TAP systems will be operating at BOS and DTW. The FAA Terminal Area Fore-

cast predicts that the total number of operations at BOS in 2005 will be 11 percent greater than the number in 1993. As an estimate of demand in 2005, we increased each demand value in the six BOS seasonal demand patterns by 11 percent. Model results for 26 years of weather data at BOS were calculated.

We input the weather time series just described above into the capacity models using the parameters representing the five technology states. This gave five sets of capacity time series.

These capacity estimates are then input into the queue models to generate the delay estimates from the baseline cases and the three TAP implementations.

Discussion

The results show that the pattern of estimated relative benefits from the TAP technologies is quite consistent over 26 years of varying weather. Implementing only the TAP 1 technologies in 2005 would recover about half the increase in delay occasioned by going to 2005 demand levels with only the capacity improvements to be expected from planned CTAS implementations. That is, this implementation would lead to about an 9 percent increase in delays over 1993 levels.

Implementing the TAP 2 technologies by 2005 would give a substantial decrease in IMC delays over 1993 levels, of about 22 percent. Implementing the TAP 3 technologies would reduce IMC delays yet more significantly, by about 60 percent (i.e., this would bring delays on IMC days to about 40 percent of 1993 levels).

RESULTS AT BOS FOR 2015

This section describes our method of modeling effects of the TAP technologies at BOS in 2015.

Weather Data

Because the year-to-year results for 2005 implementations scatter so little, we estimated the results of implementations in 2015 from weather data for a single, typical year rather than by repeating the analyses for all 26 years. We chose 1982 for the representative year, because that year's five values of IMC delays for current, 2005, TAP 1, TAP 2, and TAP 3 conditions are closest to the 26-year means of these results. We prefer to use the weather of an actual year rather than some average of the 26-year weather data, because the averaging might construct implausible weather data.

Demand Data

Demand data for 2015 were generated by growing the year 2005 demand at rates prescribed in the FAA Terminal Area Forecast (TAF) for the years 2001 to 2005. The TAF shows BOS operations growing at an essentially constant rate of 1.5 percent per year. Applying 10 years growth at the average of the 2001 to 2005 rates to the TAF 2005 operations forecast leads to an estimate of 2015 demand that is 29 percent greater than the 1993 demand. Accordingly, to estimate 2015 demand, we applied a 29 percent increase to the six representative seasonal demand patterns used to analyze BOS.

The 2015 demand data were input into the BOS capacity model. Table 5-9 displays the results for 2015 along with the results for current and 2005 baseline conditions (based on 1982 weather year).

Table 5-9. Annual Aircraft Arrival Delay at BOS (Millions of Minutes)

Technology State	1993	2005	2015
Current	5.5	6.8	12.2
TAP 1	–	5.9	10.8
TAP 2	–	4.8	8.9
TAP 3	–	2.1	4.2

MODEL RESULTS AT DTW

This section describes our results for DTW.

Weather Data

Because the results for 26 years at BOS varied so predictably with weather, we decided to identify a representative year of weather data for DTW and treat that year. The mean number of hourly reports of IMC at DTW for the 20 years 1971 to 1990 is 1,157. The year 1985 was close to that value, and that year of weather data was used as the weather input for DTW.

Demand Data

We based the demand data for 2005 and 2015 on the demand profiles used for the baseline estimates. As with BOS, we estimated future demand at DTW using data from the FAA TAF. For 2005 patterns, we multiplied each demand value in our three patterns by the ratio of total operations forecast for DTW in 2005, to that same number for the year 1995. The TAF forecast shows total operations at DTW increasing by roughly 1.5 percent annually for 2000 to 2005. To estimate total operations in 2015, we continued this rate of growth. The TAF predicts a 22 percent increase in total operations at DTW from 1995 to 2005. Our extrapolation of the TAF predictions leads to an estimate of a 36 percent increase from 1995 to 2015.

We input the weather data to our DTW capacity model, for each of five parameter sets representing technology in 1995, in 2005, and in 2015 with TAP 1, TAP 2, and TAP 3 implementations. We then used the resulting capacity time series with demand time series just described, to estimate aircraft-minutes of delay at DTW for the five technology states. Table 5-10 shows the results.

Table 5-10. Aircraft Delay at DTW for TAP Implementations (in Millions of Minutes)

	Current Reference 1995	2005	2015
Baseline	1.1	1.6	2.8
TAP 1	–	1.5	2.6
TAP 2	–	1.4	2.0
TAP 3	–	1.1	1.4

Discussion

The models indicate that DTW experiences significantly less delay than BOS. This result is consistent with the relative frequency of delays currently experienced at these two airports: The ratio of the predicted total delay at BOS to total delay at DTW in current conditions is roughly 4:1. This is also the ratio implied by delay data in the 1994 *FAA System Capacity Report.*

The reason for the difference is not that DTW has less IMC than BOS; in fact, it has more, as shown by the discussions in Chapter 2. Nor is it the reason that DTW has less traffic; while DTW had about 20 percent less traffic than BOS in 1993, operations at DTW are forecast to increase faster than at BOS. In 2005 and 2015, DTW is forecast to have slightly more operations than BOS. The principal reason for the dif-

ference is that the parallel runways at DTW are sufficiently widely spaced that they can continue independent operations in IMC, while that is not the case at BOS. Thus BOS loses much more capacity in IMC than does DTW.

The analysis shows that the TAP systems should reduce delay at DTW, but not as much as at BOS. The reason for this appears to be that delays at BOS are largely due to bad days on which demand significantly exceeds capacity for substantial parts of the day while there are much fewer such days at DTW. TAP is more effective on those bad days than on the ordinary days, and ordinary days are more important to delay at DTW than at BOS.

Chapter 6
Converting Estimated Delays Into Air Carrier Costs

This chapter details how the costs of the delays were determined.

SOME DEFINITIONS

Direct operating costs (DOCs) include flight crew costs (e.g., salaries, benefits/pensions, payroll taxes, and personnel/training expenses); fuel and oil costs (including taxes); maintenance costs (including maintenance overhead); insurance and injuries/loss/damage charges; aircraft rentals; and aircraft depreciation/amortization charges.

Variable operating costs (VOCs) are DOCs *minus* aircraft rentals and aircraft depreciation/amortization charges. Aircraft rentals and depreciation/amortization are excluded from VOC because they reflect the passage of time (and hence are sometimes called period costs) rather than how intensively and/or efficiently aircraft are operated.

Block time is measured from when the aircraft first moves under its own power at the departure airport until it comes to rest at the arrival airport. Block time is therefore more inclusive than flight time, which is measured from takeoff to landing.

FORM 41 DATA

Data collected by the Department of Transportation (DOT) from major, national, and large regional airlines at the equipment level of detail cover substantially all of the scheduled passenger traffic that occurs in the United States.

Using actual cost and traffic data for this analysis has the advantage of capturing how airframe/engine combinations are actually used by the airlines and the resources consumed to operate them that way. The actual data also reflect the effects of factors such as airline routing/scheduling decisions and airport/airspace congestion.

For the purposes of this analysis, we subdivided commercial passenger aircraft into three categories: turboprops, short-haul jets, and long-haul jets. A 1,000 mile average stage length (ASL) range is a fairly natural breakpoint for short- versus long-haul jet

aircraft. The most important cost and operating statistics for these three groups of aircraft are summarized in Table 6-1.

Table 6-1. Passenger Airline Operating Statistics

Category	Share of Direct Operating Costs (%)	Share of Variable Operating Costs (%)	Share of Fuel Costs (%)	Share of ASMs Flown (%)	Share of RPMs Flown (%)	Average Seats per Aircraft	Average Stage Length (miles)
Turbo-props	1.9	1.6	0.9	0.7	0.6	33	179
Short-haul jets	53.4	54.3	50.9	48.1	45.2	131	580
Long-haul jets	44.7	44.1	48.2	51.2	54.2	246	1,653

As shown in Table 6-1, turboprops and short-haul jets consume a higher proportion of total costs relative to their shares of revenue passenger miles flown. This occurs for several reasons. Because short-haul flights spend relatively less time at cruise at efficient conditions compared with the higher costs (in time and fuel) of—taking off, maneuvering out of the departure terminal area, climbing to altitude, maneuvering into the arrival terminal area, and landing—their relative costs are higher than long-haul flights. Second, load factors on turboprops and short-haul jets are lower than for long-haul jets (51.6 percent and 59.8 percent versus 67.3 percent, respectively).

It is also important to note the positive correlation between average seats per aircraft and the average stage lengths flown. Consequently, the higher the proportion of short-haul flights into an airport, the larger will be the expected share of turboprops and smaller jet aircraft.

ESTIMATED SYSTEM-WIDE DELAY COSTS PER BLOCK MINUTE

To estimate upper and lower bounds for system-wide delay costs per block minute, we defined pessimistic and optimistic scenarios. For the pessimistic scenario, we added an allocated share of cabin crew costs to the reported equipment-level DOC and divided by block minutes of time. This estimate of delay cost includes fuel costs plus aircraft depreciation/amortization and rental costs. It therefore implicitly assumes that all arrival delay is incurred in the air and that some incremental capital costs are incurred during the delay period. For the optimistic scenario, we started

with VOC (therefore excluding aircraft depreciation/amortization and rental costs), once again added an allocated share of cabin crew costs, *subtracted* fuel costs, and divided by block minutes of time. This estimate implicitly assumes that all arrival delay is incurred on the ground (where consumption of fuel is much lower than in the air) and that depreciation/amortization and rental costs would have to have been paid whether the aircraft was productively employed or not and therefore should not be charged against the delay. It is therefore appropriate to think of these two scenarios as the upper and lower bounds, respectively, on the true costs of aircraft delay experienced by the airlines. No attempt was made to estimate the costs to the airlines or the flying public resulting from canceled flights. Estimated system-wide delay costs per block minute are summarized in Table 6-2.

Table 6-2. System-wide Delay Costs by Type of Aircraft

Type of Aircraft	Pessimistic Case: Direct operating costs + cabin crew cost ÷ by block time ($)	Optimistic Case: Variable operating costs + cabin crew cost - fuel cost ÷ by block time ($)
Turboprop	11.09	6.15
Short-haul jet	35.36	20.29
Long-haul jet	68.94	36.73
Weighted average	43.26	24.01

OPERATIONS AT BOSTON'S LOGAN INTERNATIONAL AIRPORT AND DETROIT'S WAYNE COUNTY AIRPORT

In order to gain insights into the composition and significance of the various types of aircraft that are flown into the Boston Logan and Detroit Wayne County airports, we extracted scheduled flight data for January 1993 from the Official Airlines Guide (OAG) North American and Worldwide merge files. These data sources are computer tapes that list all of the flights that were scheduled to occur during a certain period of time, listed by carrier and type of equipment. The OAG flight data were combined with DOT Form 41 load factor and stage length statistics to estimate the number of passengers and revenue-passenger miles flown. Summary results are shown in Tables 6-3 and 6-4.

Table 6-3. Operations at Boston, Logan Airport

Type of Aircraft	Arrivals (% of total)	Passengers (% of total)	Revenue Passenger Miles (% of total)
Turboprop	44.1	10.0	1.8
Short-haul jet	42.8	56.0	35.1
Long-haul jet	13.1	34.0	63.1

Table 6-4. Operations at Detroit, Wayne County Airport

Type of Aircraft	Arrivals (% of total)	Passengers (% of total)	Revenue Passenger Miles (% of total)
Turboprop	23.5	5.1	0.9
Short-haul jet	64.1	66.5	41.5
Long-haul jet	12.4	28.4	57.6

It is interesting to note the turboprops' disproportionate shares of arrivals relative to passengers transported and revenue-passenger miles flown at both airports. Turboprop flights are particularly prevalent at Boston. Conversely, long-haul jets represent relatively fewer arrivals but much higher proportions of the RPMs flown at both airports.

Arrival Delay Costs at Boston's Logan International Airport and Detroit's Wayne County Airport

It is possible to estimate upper and lower bounds on arrival delay costs at the Boston and Detroit airports that reflect their individual flight compositions. The results are shown in Table 6-5. According to these estimates, aggregate airline costs per minute of arrival delay are lower at both airports compared with the system-wide averages. This effect occurs because of the relatively high proportions of turboprop flights, particularly at Boston's Logan airport.

Table 6-5. Airport-Specific Cost per Minute of Arrival Delay

Airport	Arrival delay cost per minute, upper bound ($)	Arrival delay cost per minute, lower bound ($)
Boston, Logan	29.06	16.21
Detroit, Wayne County	33.82	19.01
System-wide	43.26	24.01

POTENTIAL SAVINGS FROM TAP TECHNOLOGIES

As described in Chapter 4 of this report, when the level of operations is combined with the airport capacity (which is itself affected by technology and weather), the LMI Airport Capacity Model yields reliable predictions of arrival delay experienced by the airlines. As shown in Table 6-6—given the 1993 level of airport operations, a year's worth of representative weather, and existing technology—the predicted levels of arrival delay measured in aircraft minutes are 5.5 million and 1.1 million for Boston and Detroit, respectively. Because of relatively modest growth to the year 2005 in airport operations at Boston, arrival delay is expected to grow there at a much slower rate compared with Detroit. From 2005 to 2015, however, the compound growth rates of arrival delay are predicted to be 6.0 percent and 5.7 percent for Boston and Detroit, respectively.

Table 6-6. Aircraft Minutes of Arrival Delay

Airport	1993	2005	2015	Compound growth rate, 2005 to 2015 (%)
Boston	5,548,684	6,786,192	12,194,081	6.0
Detroit	1,104,555	1,614,681	2,806,667	5.7

Using the arrival delay cost factors discussed previously, it is possible to convert predicted aircraft-minutes of arrival delay into airline costs. For Boston in 1993, these arrival delay costs are estimated at between $89.9 million and $161.2 million, while at Detroit in 1993, the lower and upper bounds are $21.0 million and $37.4 million. Airline arrival delay costs grow modestly to the year 2005, but accelerate quite dramatically thereafter. By 2015, predicted airline arrival delay costs at these two airports are expected to more than double from the 1993 levels, holding technology constant.

Table 6-7. Airline Arrival Delay Costs
($ Millions)

Airport	1993	2005	2015
Boston, upper bound	161	197	354
Boston, lower bound	90	110	198
Detroit, upper bound	37	55	95
Detroit, lower bound	21	31	53

If TAP technologies ultimately prove to be successful and are implemented by the year 2005, the LMI Airport Capacity Model predicts that there will be significant improvements in airport capacity at the Boston and Detroit airports, particularly during periods of inclement weather. Consequently, certain proportions of predicted arrival delay are avoided as the TAP increments are progressively added. By multiplying the predicted reduction in aircraft-minutes of arrival delay times the airport-specific delay cost factors, yearly benefits in terms of reduced airline arrival delay costs can be estimated for each year from 2005 to 2015. Using a 5 percent real interest rate, these future benefits can be discounted back to the present so that they may be compared with the costs of the TAP program. We use a real interest rate (as opposed to a nominal one) because future benefits are measured in constant 1995 dollars. We selected a 5 percent interest rate because of the risk of R&D investments and the uncertainty of future payoffs. As shown in Table 6-8, the biggest payoffs at Boston and Detroit are from TAP Increments 2 and 3.

Table 6-8. Present Value of Arrival Delay Costs Avoided ($ Millions)

Airport	TAP Increment 1	TAP Increment 2	TAP Increment 3	Total
Boston, upper bound	165	236	542	937
Boston, lower bound	92	129	302	523
Detroit, upper bound	24	62	70	157
Detroit, lower bound	14	35	39	88

ADDITIONAL DATA NEEDED

The conclusions of the analysis appear to be robust with respect to the effects of weather variations and the results are consistent with delays currently experienced at the two airports. However, the following additional analysis and data collection would benefit the analysis;

1. The available data on arrival runway occupancy time are sparse and too unreliable to provide consistent insight into current operations, much less the impact of advanced technologies. NASA and the FAA should collaborate under the LVLASO program to collect arrival ROT data during peak traffic operations under VMC and IMC conditions. While this study shows that ROT will be a significant constraint as arrival separation distances shorten, the study cannot clearly identify at what point the constraint will be binding without better ROT data.

2. The effects of CTAS and CTAS-FMS integration on the distribution of interarrival time are important and field data from the ongoing CTAS tests should be made available as they are generated. These real-world experiments will provide useful insights into the potential impact of the TAP program.

3. This study did not address the technical feasibility of the systems being developed under the TAP program. All the benefits estimated assume the successful development and implementation of the TAP systems. Further research into the technical and cost risk of these systems would be valuable to the TAP program managers as the TAP program evolves.

4. The study did not include any benefits from increasing capacity during IMC conditions for dependent parallel runways. The parallel runways at DTW are sufficiently far apart that they operate independently during IMC. Boston Logan, with its parallel runways separated by only 1500 feet, might potentially gain enormous increases in capacity during IMC if they could be operated independently. At this time, however, the feasibility of operating runways that closely spaced is too uncertain for the possible benefits to be included in this analysis. The exclusion of those benefits is not meant to imply that we concluded that independent operations are unachievable at BOS. The possible benefits are enormous, and more research is required to determine whether the technical goals are feasible.

5. Full estimates of TAP benefits require modeling interactions between delayed arrivals and subsequent departures at a single airport, and a network analysis of the National Airspace System using evolving conditions.

CONCLUSIONS

These are the major conclusions of the study:

1. It is possible to construct parametric models with parameters that can be adjusted to reflect various stages of implementation of the TAP technologies that give the capacities of specific airports as functions of meteorological conditions, such that air traffic controllers experienced at the airports, agree with the models' predictions.

2. Impacts of the TAP technologies on delays will vary significantly from airport to airport, even among airports with similar arrival demand and delay-producing weather features. This is the case for BOS and DTW; here the distinguishing feature is the fact that BOS loses key runways in IMC because of close runway spacing, while DTW does not.

3. For the two airports examined in detail, Boston's Logan and Detroit's Wayne County, the estimated costs to the airlines from arrival delay are already significant. For 1993, arrival delay costs to the airlines operating at Boston are estimated at between $90 million and $161 million, while at Detroit the lower and upper bounds on estimated arrival delay costs are $21 million and $37 million. Because of expected growth in the number of operations at both airports, arrival delay costs at both airports are expected to more than double by the year 2015. If the value of passenger time is added to these direct benefits, the potential savings would be much greater.

4. If TAP technologies ultimately prove to be successful and are implemented by the year 2005, we predict that there will be significant improvements in airport capacity at the Boston and Detroit airports, particularly during periods of inclement weather. As a consequence, the airlines flying into these two airports are expected to save on their operating costs from reduced aircraft-minutes of arrival delay. The present value of airline cost savings projected at Boston for the years 2005 to 2015 is between $523 million and $937 million. For Detroit, the present value of the airline savings is between $88 million and $157 million.

Appendix A
Statistics of Interarrival and Interdeparture Times and the LMI Runway Capacity Model

OPERATING CASES MODELED

In this section, we develop detailed models of runway operations and capacities. The parameters that we will use are identified in Table A-1.

Table A-1. Key Airport Modeling Parameters

Symbol	Definition
c	Communication time delay
δc	Variation in c
D	Length of common approach path
p_i	Fraction of operating aircraft that are type I
Ra_i	Arrival runway occupancy time of ith aircraft
δRa_i	Variation in Ra_i
Rd_i	Departure runway occupancy time of ith aircraft
δRd_i	Variation in Rd_i
S	Miles-in-trail separation minimum
V_i	Approach speed of aircraft I
δV_i	Variation in approach speed of aircraft I
δW_i	Wind variation experienced by aircraft I
δX_i	Position uncertainty of aircraft I
μ	Time increment imposed by controller

We will assume that each of the δc, δRD_i, δRA_i, δVi, δWi, and δXi are independent normal random variables with mean zero and standard deviation σ_c , σ_{RDi} , σ_{RAi} , σ_{Vi} , σ_{Wi} , or σ_{Xi} as appropriate.

In the following we take a "controller-based view" of operations. That is, we assume that a person controls the aircraft, introducing time (or, equivalently, space) increments in operations streams to meet all applicable rules (e.g., miles-in-trail requirements) with specified levels of confidence. For example, consider the arrival-arrival sequence of Figure A-1.

Figure A-1. Time Phase for Arrivals when Follower Velocity > Leader Velocity

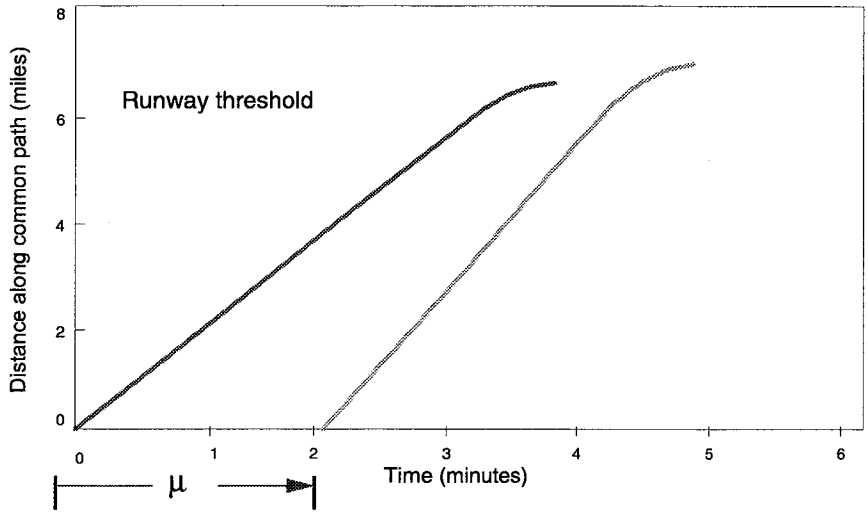

Figure A-1 shows the space-time trajectories of two arrivals. Zero distance is the beginning of the common approach path. In this model, the controller maneuvers the following aircraft so that it enters the common approach path a time μ after the lead aircraft enters it. (The controller may actually achieve this by bringing the following aircraft onto the common path when the lead aircraft has advanced a specified distance along the path.) The controller chooses the time interval μ in light of his/her knowledge of typical approach speeds for the two aircraft, as well as knowledge of disturbances affecting their relative positions—winds, position uncertainties, variations in pilot technique—in order to ensure that miles-in-trail requirements and runway occupancy rules are met, with assigned levels of confidence. As we will see shortly, this action of the controller, together with information on statistics of aircraft operating parameters and the disturbances to arrival operations, such as winds and position uncertainties, leads directly to statistics of operations and of runway capacity.

Arrivals only

We consider first the controller-based paradigm, for the case of arrivals only. Two cases are important. The first, illustrated by Figure A-1, occurs when the mean approach speed of the following aircraft exceeds that of the leader.

FOLLOWER VELOCITY ≥ LEADER VELOCITY

For this case, the miles-in-trail constraint (distance) applies as the leader crosses the runway threshold. At that time, the leader's position is D. We will derive a condition on the controller's interval μ, to guarantee that the miles-in-trail requirement is met (i.e., that at the time the leader crosses the threshold, the follower is at least distance S away from the threshold, with a probability of 95 percent).

The position of the lead aircraft is given by

$$X_L = \delta X_L + (V_L + \delta V_L + \delta W_L)t \qquad \text{[Eq. A-1]}$$

and the position of the following aircraft by

$$X_F = \delta X_F + (V_F + \delta F_F + \delta W_F)(t - \mu) \qquad \text{[Eq. A-2]}$$

The leader crosses the runway threshold at time t_{LO}, given by

$$t_{LO} = \frac{D - \delta X_L}{V_L + \delta V_L + \delta W_L} \qquad \text{[Eq. A-3]}$$

At time t_{LO}, the follower is at $X_F(t_{LO})$, given by

$$X_F(t_{LO}) = \delta X_F + (V_F + \delta V_F + \delta W_F)\left(\frac{D - \delta X_L}{V_L + \delta V_L + \delta W_L} - \mu\right) \qquad \text{[Eq. A-4]}$$

We wish to derive a condition on μ, to make $D - X_F(t_{LO}) \geq S$, with probability at least 95 percent. To keep the problem tractable, we will assume that all disturbances are of first order and linearize equation A-4. When linearized, A-4 becomes

$$X_F(t_{LO}) = \delta X_F + \frac{DV_F}{V_L}\left(1 + \frac{\delta V_F + \delta W_F}{V_F} - \frac{\delta X_L}{D} - \frac{\delta V_L + \delta W_L}{V_L}\right) - \mu V_F\left(1 + \frac{\delta V_F + \delta W_F}{V_F}\right) \qquad \text{[Eq. A-5]}$$

In this linear approximation, $X_F(t_{LO})$ is a normal random variable of mean $\frac{DV_F}{V_L} - \mu V_F$ and variance

$$\sigma_1^2 = \frac{D^2 V_F^2}{V_L^2}\left(\frac{\sigma_{VF}^2 + \sigma_{WF}^2}{V_F^2} + \frac{\sigma_{XL}^2}{D^2} + \frac{\sigma_{VL}^2 + \sigma_{WL}^2}{V_L^2}\right) + \mu^2 V_F^2 \frac{\sigma_{VF}^2 + \sigma_{WF}^2}{V_F^2} + \sigma_{XF}^2 \quad \text{[Eq. A-6]}$$

The condition that $D - X_F(t_{LO}) \geq S$, with probability at least 95 percent, may then be stated as

$$\frac{DV_F}{V_L} - \mu V_F + 1.65\,\sigma_1 \leq D - S \quad \text{[Eq. A-7]}$$

or

$$\mu \geq \frac{D}{V_L} - \frac{D-S}{V_F} + \frac{1.65\sigma_1}{V_F} \quad \text{[Eq. A-8]}$$

Equation A-7 gives, in essence, the desired condition. As that equation stands, μ appears on both sides of the inequality. Straightforward manipulations lead to an explicit condition on μ, which may be written

$$\mu \geq \frac{A + \sqrt{A^2B^2 + C^2(1-B^2)}}{1-B^2} \quad \text{[Eq. A-9]}$$

where

$$A \equiv \frac{D}{V_L} - \frac{D-S}{V_F} \quad \text{[Eq. A-10]}$$

$$B^2 \equiv 1.65^2\left\{\frac{\sigma_{VF}^2 + \sigma_{WF}^2}{V_F^2}\right\} \quad \text{[Eq. A-11]}$$

and

$$C^2 \equiv \frac{1.65^2}{V_F^2}\left\{\frac{D^2 V_F^2}{V_L^2}\left(\frac{\sigma_{VF}^2 + \sigma_{WF}^2}{V_F^2} + \frac{\sigma_{XL}^2}{D^2} + \frac{\sigma_{VL}^2 + \sigma_{WL}^2}{V_L^2}\right) + \sigma_{XF}^2\right\} \quad \text{[Eq. A-12]}$$

To determine numerical values of the smallest μ that meet A-7, the iterative scheme

$$\mu_{n+1} = \frac{D}{V_L} - \frac{D-S}{V_F} + \frac{1.65\sigma_1(\mu_n)}{V_F}$$

where $\sigma_1(\mu)$ is defined by A-6, is convenient.

Now, let us develop a condition on μ that will guarantee that the follower aircraft does not cross the runway threshold until the leader has left the runway, with probability 98.7 percent. The leader will exit the runway at time $t_{LO} + RA_L$, and the follower will cross the threshold at time t_{FO}, given by

$$t_{FO} = \frac{D - \delta X_F}{V_F + \delta V_F + \delta W_F} + \mu \qquad \text{[Eq. A-13]}$$

Linearizing as above, we find that in the linear approximation t_{FO} - t_{LX} is a normal random variable with mean $\frac{D}{V_F} + \mu - \frac{D}{V_L} - \overline{RA}_L$, where $\overline{RA}_L$ denotes the mean of RA_L and variance

$$\sigma_2^2 = \frac{D^2}{V_F^2}\left(\frac{\sigma_{XF}^2}{D^2} + \frac{\sigma_{VF}^2 + \sigma_{WF}^2}{V_F^2}\right) + \frac{D^2}{V_L^2}\left(\frac{\sigma_{XL}^2}{D^2} + \frac{\sigma_{VL}^2 + \sigma_{WL}^2}{V_L^2}\right) + \sigma_{RAL}^2 \qquad \text{[Eq. A-14]}$$

It follows that the condition on μ for the follower not cross the threshold until the leader has exited the runway. That is, t_{FO} - $t_{LX} > 0$ with probability 98.7 percent is

$$\mu \geq \frac{D}{V_L} - \frac{D}{V_F} + \overline{RA}_L + 2.215\sigma_2 \qquad \text{[Eq. A-15]}$$

The controller will, in effect, impose that value of time interval μ that is the smallest μ satisfying both A-7 and A-14.

Given μ, the time between threshold crossings of successive arrivals is, in our approximation, a normal random variable of mean

$$\frac{D}{V_F} - \frac{D}{V_L} + \mu \qquad \text{[Eq. A-16]}$$

and variance

$$\sigma_3^2 = \frac{D^2}{V_F^2}\left(\frac{\sigma_{XF}^2}{D^2} + \frac{\sigma_{VF}^2 + \sigma_{WF}^2}{V_F^2}\right) + \frac{D^2}{V_L^2}\left(\frac{\sigma_{XL}^2}{D^2} + \frac{\sigma_{VL}^2 + \sigma_{WL}^2}{V_L^2}\right) \quad \text{[Eq. A-17]}$$

FOLLOWER VELOCITY < LEADER VELOCITY

When the follower's approach speed is slower than the leader's, in the controller-based view the controller will bring the follower onto the common path after the leader has advanced a distance S along it, as illustrated in Figure A-2.

Figure A-2. Time Phase of Arrivals when Follower Velocity < Leader Velocity

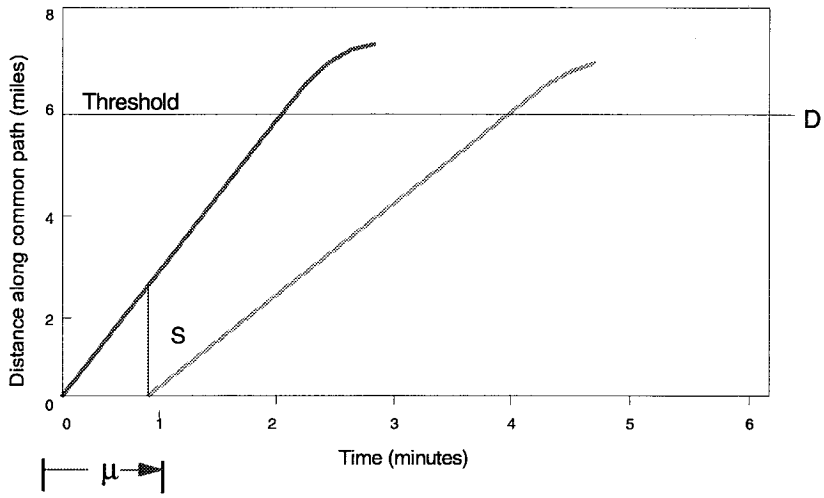

In this case, the positions of the two aircraft as functions of time are again given by A-1 and A-2. The miles-in-trail requirement is now, that $X_L(\mu) - X_F(\mu) \geq S$, with probability at least 95 percent. As

$$X_L(\mu) - X_F(\mu) = \delta X_L + (V_L + \delta V_L + \delta W_L)\mu - \delta X_F \quad \text{[Eq. A-18]}$$

is a normal random variable of mean $V_L\mu$ and variance

$$\sigma_4^2 = \mu^2(\sigma_{VL}^2 + \sigma_{WL}^2) + \sigma_{XF}^2 + \sigma_{XL}^2 \quad \text{[Eq. A-19]}$$

it follows that the condition that the miles-in-trail requirement is met, with 95 percent confidence, is

$$\mu \geq \frac{S}{V_L} + 1.65\frac{\sigma_4}{V_L} \qquad \text{[Eq. A-20]}$$

Equation A-19 may be written as a single condition on μ using equation A-8 by replacing equations A-9, A-10, and A-11 with the new definitions

$$A \equiv \frac{S}{V_L}$$

$$B^2 \equiv 1.65^2 \frac{\sigma_{VL}^2 + \sigma_{WL}^2}{V_L^2}$$

$$C^2 \equiv 1.65^2 \frac{\sigma_{XL}^2 + \sigma_{XF}^2}{V_L^2}$$

The condition that the single-occupant rule is met with 98.7 percent confidence is derived exactly as is that condition for $V_F \geq V_L$ (i.e., condition A-14). In the present case, too, the result is given by equation A-14. Also, in the present case, equations for the mean and standard deviation of IAT, given μ, are given by A-15 and A-16.

ARRIVAL-DEPARTURE-ARRIVAL-DEPARTURE SEQUENCES

We can readily translate the results of the previous section to results for repeated A-D operations by replacing RA_L with $RA_L + RD_D$, where the subscript D denotes the intervening departure aircraft. This case is illustrated by Figure A-3.

Figure A-3. Time Phase of Arrivals with Intervening Departure

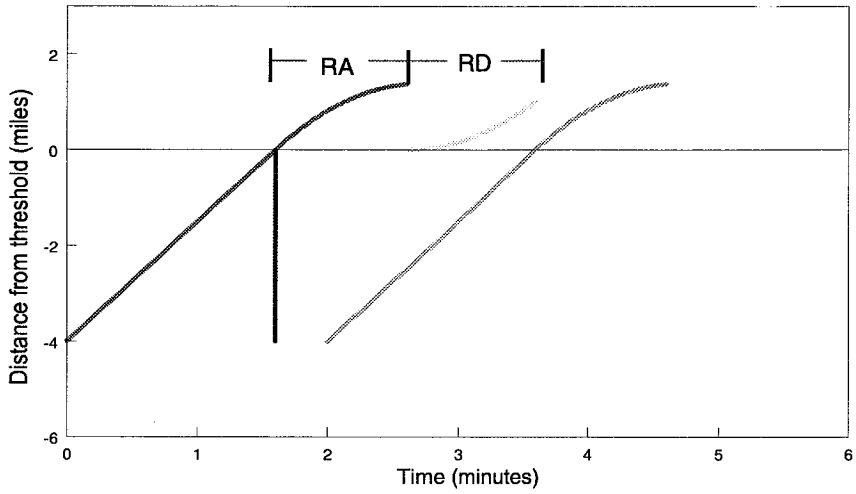

It may be desirable to consider the effect of a communications lag c on the departure. If so, then RA_L is replaced by $RA_L + c + RD_D$.

Statistics of Multiple Operations

At this point, we have expressions for the means and variances of normal random variables representing interarrival times for a variety of cases. Now we wish to use these, to generate statistics of multiple arrivals, or multiple arrivals and departures, to produce capacity curves for single runways and combinations of runways.

First, we consider the statistics of sequences of arrivals only. Statistics of the overall interarrival time will be determined by the mix of aircraft using the runway, with their individual values of the aircraft parameters of Table A-1. Suppose three aircraft types use the runway, and the fraction of the aircraft of type i in the mix is p_i. The previous results give interarrival time for each pair as a normal random variable. Let the mean and standard deviation for aircraft type i following aircraft type j be μ_{ij} and σ_{ij}, respectively. Then the distribution function for overall interarrival time is

$$p_{AA}(t) = \sum_i \sum_j p_i p_j N(t;\mu_{ij},\sigma_{ij}) \qquad \text{[Eq. A-21]}$$

where N(t; μ, σ) denotes the normal probability distribution function. Obviously, the distribution of interarrival times is not normal. An example of an interarrival time distribution of the type A-21 is shown in Figure A-4.

Figure A-4. Interarrival Time (Distribution)

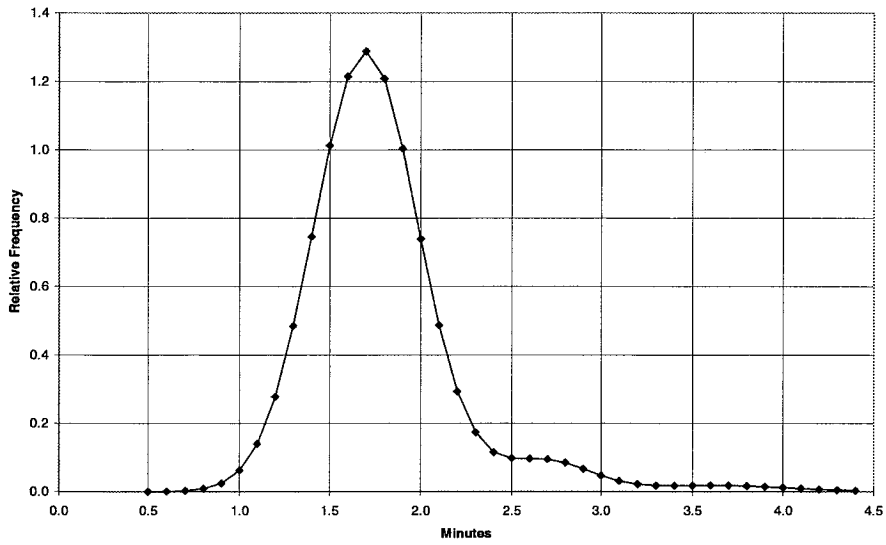

As Figure A-4 shows, the interarrival time distribution is not necessarily monomodal.

One can compute the mean and variance of the interarrival time distribution, A-21, straightforwardly: The results are

$$< t_{AA} >= \sum_i \sum_j p_i p_j \mu_{ij} \qquad \text{[Eq. A-22]}$$

and

$$\text{var}(t_{AA}) = \sum_i \sum_j p_i p_j (\sigma_{ij}^2 + \mu_{ij}^2) - < t_{AA} >^2 \qquad \text{[Eq. A-23]}$$

In principle, one can compute exactly the distributions of total arrival times for A-A-A sequences of arbitrary length and find exact values for the number of arrivals that can, with assigned confidence, be accommodated in 1 hour. These calculations in-

volve sums of many terms, however, and this motivates a search for useful approximations.

Sums of normal random variables are normally distributed, and it is tempting to approximate the distribution of sequences of many arrivals in such a way. An A-A-A... sequence with J_{ij} cases of aircraft of type i following aircraft of type j has a normal distribution whose parameters are easily computed. If one could choose the J_{ij} so that $J_{ij} = p_i p_j M$, where M is the sum of the J_{ij} , then the resulting normal distribution would be a good approximation for the distribution of long arrival sequences. Unfortunately, for the aircraft mixes at some airports, some of the p_i are only a few hundredths, so M would have to be several thousand for this approximation to be accurate.

Nevertheless, because much of our work to this point has been approximate, it does not seem unreasonable to consider this "very large sequence"-limiting case. In this approximation, then, the time t_M of M interarrival times has a normal distribution of mean $M\langle t_{AA}\rangle$ and variance

$$\mathrm{var}(t_M) = M \sum_i \sum_j p_i p_j \sigma_{ij}^2 \qquad \text{[Eq. A-24]}$$

This result suggests approximating the distribution of interarrival time with a normal distribution of mean $\langle t_{AA}\rangle$ and variance v_1 given by

$$v_1 = \sum_i \sum_j p_i p_j \sigma_{ij}^2 \qquad \text{[Eq. A-25]}$$

It may be more appropriate to use the approximation v_1 as an input for the variance of interarrival time in the FAA Airfield Capacity Model than the actual variance given in A-23. This is because that model appears to use the IAT variance in computing properties of sequences of large numbers of operations.

We can use the approximation of A-25 to compute the number of arrivals that can be accommodated in 1 hour with 95 percent confidence. That number M is determined by the condition $(M-1) < t_{AA} > +1.65\sqrt{(M-1)v_1} \leq 60$ (only M-1 interarrival times are required for M arrivals)[13], which leads to the all-arrival capacity of a single runway as $M^* = w^2 + 1$, where w is given by

$$w = -\frac{1.65\sqrt{v_1}}{2 < t_{AA} >} + \sqrt{\left(\frac{1.65\sqrt{v_1}}{2 < t_{AA} >}\right)^2 + \frac{60}{< t_{AA} >}}$$

To compute the expected number of arrivals we use

$$\overline{M} = 60 / < t_{AA} >$$

RUNWAY CAPACITY CURVE

At this point, we have one point on the single-runway capacity curve, the one corresponding to all arrivals and no departures. We can generate others.

The distribution function of Figure A-4 suggests that there is a significant probability of interarrival times large enough to accommodate a departure. We can reckon the number of "free" departures (i.e., departures that can be accommodated in a stream of $\overline{M}$ arrivals), in this way: The distribution of interarrival time is given by A-21). We assume that departure ROT, arrival ROT, and communication delay are normal random variables of means $<R_D>$, $<R_A>$, and <c> and standard deviations σ_D, σ_A, and σ_c. Thus, the distribution of the difference $t - R_D - R_A - c$, where t is the IAT, is given by

[13] This statement is accurate for any single hour considered in isolation; for a long run average, replace M-1 by M.

$$p(t - R_A - R_D - c)$$
$$= N(-< R_D > -< R_A > -< c >, \sqrt{\sigma_D{}^2 + \sigma_A{}^2 + \sigma_C{}^2}) \otimes \sum_i \sum_j p_i p_j N(\mu_{ij}, \sigma_{ij})$$
$$= \sum_i \sum_j p_i p_j N(\mu_{ij} - < R_D > -< R_A > - < c >, \sqrt{\sigma_D^2 + \sigma_{ij}^2 + \sigma_A^2 + \sigma_c^2})$$

[Eq. A-26]

where the symbol $\otimes$ denotes convolution[14]. Then the probability that t - R_D - R_A -c is positive is given by

$$p_+ = 1 - \sum_i \sum_j p_i p_j C(0, \mu_{ij} - < R_D > -< R_A > - < c >, \sqrt{\sigma_D^2 + \sigma_{ij}^2 + \sigma_A^2 + \sigma_c^2})$$

[Eq. A-27]

where C(t, μ,σ) is the normal cumulative probability function. This value is readily computed. Then one may determine the number $\overline{N}$ of positive values of t-R_D-R_A-c to be expected, in $\overline{M}$ draws, from the binomial distribution for probability p_+.

Under IMC2 or IMC3 weather conditions, current FAA procedures require that departures be held if an arriving aircraft is within a certain distance of the runway threshold. (This distance is now 2 miles.) In our model, this has the effect of reducing the time available for departing aircraft. Since the trailing arrival travels a distance less than the full length of the common path, the uncertainties embodied in A-17 are also reduced.

The appropriate modification to A-16 is to reduce the IAT by $\frac{DT}{V_F}$ where DT is the distance from threshold after which departures must be held. The variance in A-17 reduced by

[14] To account for variations in departure runway occupancy time, one may replace the single normal distribution of ROT with the distribution of departure ROT that would be found with K classes of departing aircraft, each with its own normal distribution of departure ROT. That is,

$$\sum_1^K q_i N(-< R_D >_i, \sigma_{Di})$$

where q_i denotes the fraction of departing aircraft that are of type i .

$$\frac{DT(2*D-DT)}{V_F^2}\left(\frac{\sigma_{VF}^2+\sigma_{WF}^2}{V_F^2}\right)$$

A third point on the capacity curve, the point of equal numbers of arrivals and departures, may be computed by considering sequences of repeated A-D pairs, as described in the section above.

While the expressions for interarrival times and runway capacities developed above are somewhat lengthy, they are readily evaluated numerically.

Departures

Similar considerations lead to statistics of departures. The basic departure situation is shown in Figure A-5.

Figure A-5. Time Phase of Departures

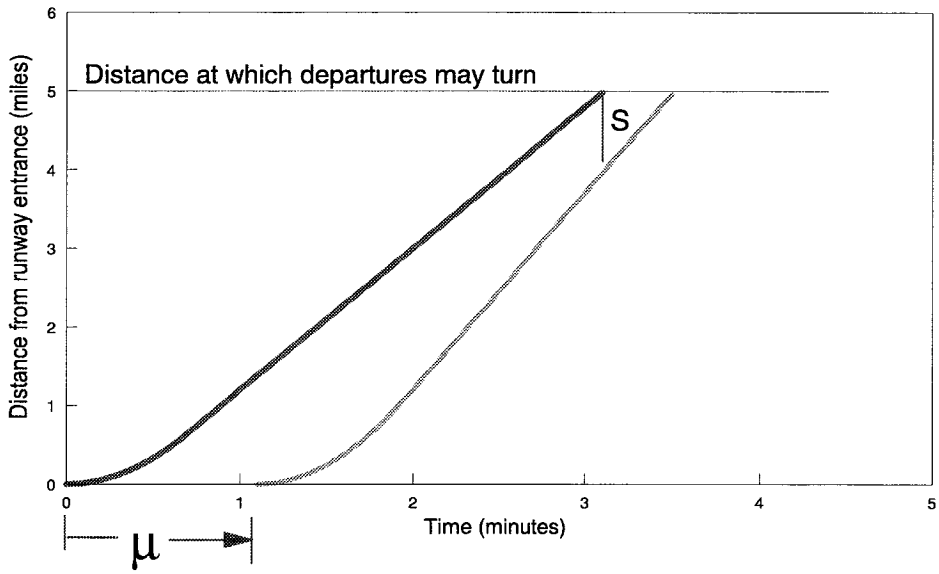

We model the trajectory of a departing aircraft by specifying its position, x(t), in terms of the parameters V_D and R_D, in this way:

$$x(t) = \begin{cases} \frac{1}{2}\frac{V_D}{R_D}t^2, 0 < t \le R_D \\ V_D t - \frac{1}{2}V_D R_D, t \ge R_D \end{cases}$$

This model approximates an actual takeoff roll and climb out by a trajectory with constant acceleration from rest to departure speed V_D, occurring in time R_D, followed by continuing departure at constant speed V_D.

We model controllers' actions on departures by the interdeparture time interval μ, which is the time interval between the start of the lead aircraft's takeoff roll to issuing a departure clearance to the following aircraft. (The following aircraft begins takeoff role at time $\mu + c$ where c models the delay to move into position) We assume that, in effect, controllers adjust μ to give specified confidence that miles-in-trail requirements, and other separation requirements, are met.

Here again, the required control input varies, depending on whether the following aircraft is faster or slower than the lead aircraft. In the case of a faster follower, the constraining condition is that the MIT requirement be met as the lead aircraft exits the system. At that time, the displacement of the lead aircraft is D_D, the distance-to-turn on departure. The displacement of the following aircraft must not be greater than $D_D - S_D$, where S_D is the minimum MIT spacing. After lengthy but straightforward steps, one finds that meeting this condition with 95 percent confidence imposes the condition

$$\mu \ge \frac{D_D}{V_{DL}} + \frac{1}{2}(R_{DL} - R_{DF}) - \frac{D_D - S_D}{V_{DF}} - c + \frac{1.65}{V_{DF}}\sqrt{\text{var}}$$

on μ. The quantity var in the inequality just above is

$$\text{var} = \left(\frac{D_D}{V_{DL}} + \frac{1}{2}(R_{DL} - R_{DF}) - \mu - c\right)^2 \left(\sigma^2_{V_{DF}} + \sigma^2_{W_F}\right) + \frac{V^2_{DF}}{V^2_{DL}} D^2_D \frac{\sigma_{VL}{}^2 + \sigma^2_{WL}}{V^2_{DL}} + \frac{V^2_{DF}}{4}\sigma^2_{RDL}$$
$$+ \frac{1}{4}V^2_{DF}\sigma^2_{RDF} + V^2_{DF}\sigma^2_C$$

The inequality may be reduced to an equivalent, explicit condition on μ. For numerical work, we find that iterative methods give the required values of μ conveniently.

When the follower departs more slowly than the leader, the MIT minima apply as the follower lifts off, unless D_D is sufficiently short that the leader can exit the system before the follower completes the takeoff roll. Applying the MIT minimum as the follower lifts off leads to the condition

$$\mu \geq \frac{R_{DL}}{2} + \left(\frac{1}{2}\frac{V_{DF}}{V_{DL}} - 1\right)R_{DF} - c + \frac{S_D}{V_{DL}} + 1.65\sqrt{\text{var1}}$$

where

$$\text{var1} = \left(\mu + c + R_{DF} - \tfrac{1}{2}R_{DL}\right)^2 \frac{\sigma^2_{V_{DL}} + \sigma^2_{WL}}{V^2_{DL}} + \left(1 - \frac{V_{DF}}{2V_{DL}}\right)^2 \sigma^2_{RDF}$$

$$+ \frac{1}{4}\left(\sigma^2_{RDL} + R^2_{DF}\frac{\sigma^2_{VDF} + \sigma^2_{WF}}{V^2_{DL}}\right) + \sigma^2_C \text{ (inequality A)}$$

Alternatively, the controller might impose a value of μ that caused the follower to lift off just as the leader exited the system. That would lead to

$$\mu \geq \frac{D_D}{V_{DL}} + \frac{1}{2}R_{DL} - R_{DF} - c + 1.65\sqrt{\sigma^2_{RDF} + \frac{D^2_D}{V^2_{DL}}\frac{\sigma^2_{V_{DL}} + \sigma^2_{WL}}{V^2_{DL}} + \frac{1}{4}\sigma^2_{RDL} + \sigma^2_C}$$

(inequality B)

Controllers would impose the less restrictive of inequality A, or inequality B. Finally, the single-occupant rule must be respected, which leads to

$$\mu \geq R_{DL} - c + 2.215\sqrt{\sigma^2_{RDL} + \sigma^2_C} \text{ (inequality C)}$$

For our model, when the follower is slower than the leader, we choose

$\mu = \max(\min(\mu_A, \mu_B), \mu_C)$,

where μ_i is the lower bound on μ resulting from inequality i.

The PASCAL code for the LMI Runway Capacity Model follows.

PASCAL CODE FOR THE LMI RUNWAY CAPACITY MODEL

```
program caplot(input,output);

{Copyright (C) 1996 Logistics Management Institute. All rights reserved.}
{This program evaluates runway capacity and mean and standard deviations}
{of interarrival time from input parameters that can be related to the }
{TAP technologies. Standard units are lengths in statute miles and times in minutes.}
{Certain input variables are given in more conventional units and converted.}
{Inputs are listed below in the const declaration.}
{A maximum of 10 a/c types can be treated with this version.}

type vec = array[1..10] of real;

var
{ variable to account for reduction in IAT window and its variance if IMC2/3}
IMC_mean, IMC_var: vec;
{ Flag set to 1 if IMC2/3}
IMC: Byte;

{ Flag set to 1 if wake vortices require 120 second separation, 0 if 60 second}
WAKE: Byte;
```

```
{Miles-in-trail for arrivals, in miles: sn[i,j] is MIT for i behind j, in}
{nautical miles.}
  sn:array[1..10,1..10] of real;
{aircraft mix:}
  p:vec;

{approach speeds, and s.d. of approach speeds, in knots:}
  vk:vec;
  sdvk:vec;

{Position uncertainties, nautical miles:}
  sdxn:vec;

{Length of common approach path, nautical miles:}
  dn:real;

{Standard deviation of wind, knots:}
  sdwk:real;

{Arrival ROT and s.d. of arrival ROT, minutes:}
  RA:vec;
  sdra:vec;
```

```
{Departure ROT and s.d. of departure ROT, minutes:}
  RD:vec;
  sdrd:vec;

{Departure speeds and s.d. of departure speeds, in knots:}
  vdk:vec;
  sdvdk:vec;

{Minimum distance before turn on departure, nautical miles:}
  ddn:real;

{Miles-in-trail for departures: assumed same as miles-in -trail for arrivals.}

{Communication delay mean and standard deviation, minutes:}
  cbar:real;
  sdc:real;

{Number of a/c types:}
  nc:integer;

{End of input data}
```

```
var
  v,sdv,vd,sdvd,sdx:vec;
  s:array[1..10,1..10] of real;
  xmu:array[0..1] of real;
  d, dd, sdw:real;

  i,j,k,l,f,m,nn:integer;
  mu1, mu2,
x0,x,rvf,rvl,s1,s2,mu,iat,sdiat,taa,sdtaa,rdbar,ssdrd,tdd,v1,v2,v3,v4,v5:real;
  pclear,qclear:real;

  {times[i,j,1] is mean iat, and times[i,j,2] is sdiat,for i behind j}
  times:array[1..10,1..10,1..2] of real;

  {Amax is max arrival rate, arrivals only; AD is max A=D rate; Dmax is }
  {max departure rate; jmax is max departures in amax arrivals.}
  abar: real;
  amax,ad,dmax:real;
  jmax:integer;

  {gov[i,j] identifies controlling constraint - MIT or ROT - for i behind j.}
  gg:string[3];
```

```
  ts:char;
  gov:array[1..10,1..10] of string[3];
  ifl,ofl:text;
  lab:string[80];

{Now load function cum(x,mu,sd:real):real, that returns cdf for normal }
{distribution at argument x, mean mu, standard deviation sd.}
{$i c:\tap\qm\cumf.pas}

function bf(x:real):real;
var
 t,vv,s, df:real;
begin {bf is difference between 95% conf of dep and cur prob using sep x}
t:=1; {t = probability starting with 1}
if IMC = 1 then df:= d-2 else df:= d;
for k:=1 to nc do
  begin
  s:=sqrt(df*df/v[f]/v[f]*(sdx[f]*sdx[f]/df/df+rvf)
       +d*d/v[l]/v[l]*(sdx[l]*sdx[l]/d/d+rvl)
       +sdra[l]*sdra[l]+sdrd[k]*sdrd[k]+sdc*sdc);
  vv:=-d/v[l]+df/v[f]-ra[l]-cbar-rd[k]+x;
  t:=t-p[k]*cum(0,vv,s)
```

```
  end;
{ Use 90% confidence on meeting slot width }
bf:=t-0.9      {find value of x that will make bf = 0 or t = 90}
end; {bf}


procedure aad;
var z:real;
begin {aad}
xmu[0]:=0;xmu[1]:=5;
if bf(xmu[0])*bf(xmu[1]) < 0
  then
    while (abs(xmu[0]-xmu[1]) > 1.e-5) do
      begin
      z:=0.5*(xmu[0]+xmu[1]);
      if (bf(xmu[0])*bf(z) < 0)
        then
          xmu[1]:=z
        else
          xmu[0]:=z
      end
  else
    writeln(f,l,k,'  Zero not bracketed');
```

```
mu2:=z;
end; {AAD}

procedure gainer;
var
  r,sd,z:real;
begin {gainer}
{The MIT mu value is determined by iteration:}
x:=d/v[l]-(d-s[f,l])/v[f];x0:=1000;
while(abs((x-x0)/x)>=1.e-6)do
  begin
  x0:=x;
  s1:=d*d*v[f]*v[f]/v[l]/v[l]*(rvf+sdx[l]*sdx[l]/d/d+rvl);
  s1:=s1+x0*x0*v[f]*v[f]*rvf+sdx[f]*sdx[f];
  x:=d/v[l]-(d-s[f,l])/v[f]+1.65*sqrt(s1)/v[f]
  end;
mu1:=x;

{Now make the mu for the single-occupancy rule condition:}
if (ts = 'A')
  then
```

```
    begin
    s2:=d*d/v[f]/v[f]*(sdx[f]*sdx[f]/d/d+rvf)
      +d*d/v[l]/v[l]*(sdx[l]*sdx[l]/d/d+rvl)
      +sdra[l]*sdra[l];
    mu2:=d/v[l]-d/v[f]+ra[l]+2.215*sqrt(s2)
    end
  else
    aad;

if(mu1 >=mu2)then mu:=mu1 else mu:=mu2;
if(mu1 >= mu2) then gg:='MIT' else gg:= 'ROT';
iat:=d/v[f]-d/v[l]+mu;
sdiat:=sqrt(d*d/v[f]/v[f]*(sdx[f]*sdx[f]/d/d+rvf)+d*d/v[l]/v[l]*(sdx[l]*sdx[l]/d/d+rvl
));
end; {gainer}



procedure looser;
var
  r,sd:real;

begin {looser}
```

```
{Here,too, we stabilize the first mu by iteration:}
x:=s[f,l]/v[f];x0:=1000;
while (abs((x-x0)/x)>1.e-6)do
  begin
  x0:=x;
  x:=s[f,l]/v[l]+1.65*sqrt(x0*x0*rvl+(sdx[f]*sdx[f]+sdx[l]*sdx[l])/v[l]/v[l]);
  end;
mu1:=x;

{Now make the mu for the single-occupancy rule condition:}
if (ts = 'A')
  then
    begin
    s2:=d*d/v[f]/v[f]*(sdx[f]*sdx[f]/d/d+rvf)
      +d*d/v[l]/v[l]*(sdx[l]*sdx[l]/d/d+rvl)
      +sdra[l]*sdra[l];
    mu2:=d/v[l]-d/v[f]+ra[l]+2.215*sqrt(s2)
    end
  else
    aad;

if(mu1 >= mu2) then mu:=mu1 else mu:=mu2;
```

```
if(mu1 >= mu2) then gg:='MIT' else gg:='ROT';

iat:=d/v[f]-d/v[l]+mu;

sdiat:=sqrt(d*d/v[f]/v[f]*(sdx[f]*sdx[f]/d/d+rvf)+d*d/v[l]/v[l]*(sdx[l]*sdx[l]/d/d+rvl
));

end; {looser}


procedure dgainer;

var

  mu1,x,x0:real;

begin {dgainer}


{Must obey single-occupant rule with 98.7% confidence.  This => one

{constraint on idt.  We tentatively assign idt this value:}

mu:=rd[l]-cbar+2.215*sqrt(sqr(sdrd[l])+sqr(sdc));


{Iterate to determine mu from MIT constraint:}

x:=dd/vd[l]+0.5*(rd[l]-rd[f])-(dd-s[f,l])/vd[f] -cbar;x0:=1000;

while(abs((x-x0)/x0)>1.e-6) do

  begin

  x0:=x;

  x:=dd/vd[l]+0.5*(rd[l]-rd[f])-(dd-s[f,l])/vd[f] -cbar;

  x:=x+1.65*sqrt((dd/vd[l]+0.5*(rd[l]-rd[f])-x0-cbar)*(dd/vd[l]+0.5*(rd[l]-rd[f])-x0-
cbar)*rvf
```

```
            +dd*dd/vd[l]/vd[l]*rvl
            +0.25*(sdrd[l]*sdrd[l]+sdrd[f]*sdrd[f])+sqr(sdc))

  end;

if (mu<x) then mu:=x;

{Now store idt in times[f,l,1]:}
times[f,l,1]:=mu+cbar;
end; {dgainer}

procedure dlooser;
var
  mua,mub,muc,mu:real;

begin {dlooser}

{Must obey single-occupant rule with 98.7% confidence.  This => one}
{constraint on idt.  We assign muc this value:}

muc:=rd[l]-cbar+2.215*sqrt(sqr(sdrd[l])+sqr(sdc));
```

```
{Iterate to determine mu from MIT constraint:}
x:=0.5*rd[l]+0.5*vd[f]/vd[l]*rd[f]-rd[f]+s[f,l]/vd[l]-cbar;x0:=1000;
while(abs((x-x0)/x0)>1.e-6) do
  begin
  x0:=x;
  x:=0.5*rd[l]+0.5*vd[f]/vd[l]*rd[f]-rd[f]+s[f,l]/vd[l]-cbar;
  x:=x+1.65*sqrt((rd[f]-0.5*rd[l]+x+cbar)*(rd[f]-0.5*rd[l]+x+cbar)*rvl
     +sdrd[f]*sdrd[f]*(1-0.5*vd[f]/vd[l])*(1-0.5*vd[f]/vd[l])
     +0.25*(sdrd[l]*sdrd[l]+rd[f]*rd[f]*vd[f]*vd[f]/vd[l]/vd[l]*rvf)
     + sdc*sdc)
  end;


mua:=x;

{Assign mub to "early turn" constraint:}

mub:= dd/vd[l]+0.5*rd[l]-rd[f]-cbar
    +1.65*sqrt(sdrd[f]*sdrd[f]+dd*dd/vd[l]/vd[l]*rvl+0.25*sdrd[l]*sdrd[l]+sdc*sdc);


{Now assign idt to max of (min(mua, mub), muc)}
```

```
if mua<mub then mu:=mua else mu:=mub;
if muc> mu then mu:=muc;
times[f,l,1]:=mu+cbar;
end; {dlooser}

procedure dequal;
var
 tmp,idt:real;
begin {dequal}
{Here, when climb-out speeds are equal, we check both the "gainer" and}
{"looser" conditions, and make idt equal to the longest of these.}
dgainer;tmp:=times[f,l,1];
dlooser; if (times[f,l,1]> tmp) then idt:=times[f,l,1] else idt:=tmp;
times[f,l,1]:=idt
end; {dequal}

begin {main}
{Get input data and set up output file:}
lab:='c:\tap\qm\capdatk1.txt';
assign(ifl,lab);reset(ifl);
lab:='c:\tap\qm\capoutk1.txt';
assign(ofl,lab);rewrite(ofl);
```

```
read(ifl,nc);nc2:=nc*nc;
for i:=1 to nc do for j:=1 to nc do read(ifl,sn[i,j]);
for i:=1 to nc do read(ifl,p[i]);
for i:=1 to nc do read(ifl,vk[i]);
for i:=1 to nc do read(ifl,sdvk[i]);
for i:=1 to nc do read(ifl,sdxn[i]);
read(ifl,dn);
read(ifl,sdwk);
for i:=1 to nc do read(ifl,ra[i]);
for i:=1 to nc do read(ifl,sdra[i]);
for i:=1 to nc do read(ifl,rd[i]);
for i:=1 to nc do read(ifl,sdrd[i]);
for i:=1 to nc do read(ifl,vdk[i]);
for i:=1 to nc do read(ifl, sdvdk[i]);
read(ifl,ddn);
read(ifl,cbar);
read(ifl,sdc);
read(ifl, IMC);
read(ifl, WAKE);

{Generate properly dimensioned distances, velocities & S. D.'s of velocities:}
```

```
{The spreadsheet GUI for this code has ALL distances in nautical miles,}
{and ALL velocities in knots.  The code uses statute miles as the standard}
{length, miles/minute as the standard speed unit, and minutes as the standard}
{time unit.}

{First, approach, departure speeds & s.d.'s of same, and pos'n uncertainties:}
for i:=1 to nc do
  begin
  v[i]:=vk[i]*6.08/5.28/60;
  sdv[i]:=sdvk[i]*6.08/5.28/60;
  vd[i]:=vdk[i]*6.08/5.28/60;
  sdvd[i]:=sdvdk[i]*6.08/5.28/60;
  sdx[i]:=sdxn[i]*6.08/5.28
  end;

{Miles-in-Trail:}
for i:=1 to nc do for j := 1 to nc do s[i,j]:=6.08/5.28*sn[i,j];

{Common path:}
D := dn*6.08/5.28;

{Wind:}
```

```
sdw:= sdwk*6.08/5.28/60;

{Distance to departure turn:}
dd := 6.08/5.28*ddn;

{Make average departure ROT and sd of average ROT, for A-D calcs:}
rdbar:=0;for i:=1 to nc do rdbar:=rdbar+p[i]*rd[i];
ssdrd:=0;for i:=1 to nc do ssdrd:=ssdrd+p[i]*(sdrd[i]*sdrd[i]+rd[i]*rd[i]);
ssdrd:=ssdrd-rdbar*rdbar;
ssdrd:=sqrt(ssdrd);
{Now make IAT statistics for each leader,follower pair, for arrivals only:}
ts:='A';
for f:=1 to nc do for l:=1 to nc do
  begin
  rvf:=(sdv[f]*sdv[f]+sdw*sdw)/v[f]/v[f];
  rvl:=(sdv[l]*sdv[l]+sdw*sdw)/v[l]/v[l];
  if (v[f] >= v[l])
  then
    gainer
  else
    looser;
  times[f,l,1]:=iat;times[f,l,2]:=sdiat;
```

```
  gov[f,l]:=gg
  end;
{Now make some overall averages}
taa:=0;sdtaa:=0;for i:=1 to nc do for j:=1 to nc do
  begin
  taa:=taa+p[i]*p[j]*times[i,j,1];
  sdtaa:=sdtaa+p[i]*p[j]*(times[i,j,2]*times[i,j,2]+times[i,j,1]*times[i,j,1])
  end;
abar:= 60/taa;
sdtaa:=sqrt(sdtaa-taa*taa);
amax:= abar;
nn:=trunc(amax);

{compute corrections ot IAT mean and variance when radar approaches}
{FAA regs require no departure if arrival within 2 miles of threshold}

if IMC=0 then for i:=1 to nc do begin IMC_mean[i]:= 0; IMC_var[i]:=0;end
else for i:=1 to nc do begin
   IMC_mean[i]:= 2/v[i]; {reduction in usable iat window}
   IMC_var[i]:= (4*(d-1)/v[i]/v[i])*((sdv[i]*sdv[i]+sdw*sdw)/v[i]/v[i]);
   {variance reductions, too}
   end;
```

```
{Now find probability of taa including a departure, on one draw:}
v1:=1;
{ Aggregate over all follower/leaders i/j and all departing classes l}


for i:=1 to nc do for j:=1 to nc do for l:=1 to nc do
  v1:=v1
  -p[i]*p[j]*p[l]*cum(0,times[i,j,1]-IMC_mean[i]-RA[j]-rd[l]-cbar,
  sqrt(times[i,j,2]*times[i,j,2]-IMC_var[i]+sdra[j]*sdra[j]+sdrd[l]*sdrd[l]+sdc*sdc));
pclear:=v1;qclear:=1-pclear;
{Now find expected number of departures that can be integrated}
{in the number of arrivals that can be done in 1 hour }
v1:=exp(nn*ln(qclear));v2:=v1;j:=0;
while (v2 <= 0.5) do
  begin
  j:=j+1;
  v1:=pclear/qclear*(nn-j+1)/j*v1;
  v2:=v2+v1
  end;
j:=j+1;
jmax:=j;
{Now consider adjusting arrival spacing so that a departure is always }
```

```
{accomodated between arrivals.  This gives a third point on the capacity curve.}
ts:='B';
for f:=1 to nc do for l:=1 to nc do
  begin
  rvf:=(sdv[f]*sdv[f]+sdw*sdw)/v[f]/v[f];
  rvl:=(sdv[l]*sdv[l]+sdw*sdw)/v[l]/v[l];
  if (v[f] >= v[l])
  then
    gainer
  else
    looser;
  times[f,l,1]:=iat;times[f,l,2]:=sdiat;
  gov[f,l]:=gg
  end;
{Now make some overall averages}
taa:=0;sdtaa:=0;for i:=1 to nc do for j:=1 to nc do
  begin
  taa:=taa+p[i]*p[j]*times[i,j,1];
  sdtaa:=sdtaa+p[i]*p[j]*(times[i,j,2]*times[i,j,2]+times[i,j,1]*times[i,j,1])
  end;
abar:= 60/taa;
sdtaa:=sqrt(sdtaa-taa*taa);
```

```
ad:= abar;
{Now deal with departures.  First, develop departure capacity for D-D-D...}

for f:=1 to nc do for l:=1 to nc do
  begin
  rvf:=(sdvd[f]*sdvd[f]+sdw*sdw)/vd[f]/vd[f];
  rvl:=(sdvd[l]*sdvd[l]+sdw*sdw)/vd[l]/vd[l];
  if (vd[f] > vd[l])
  then
   dgainer
  else
    if(vd[f] < vd[l])
    then
      dlooser
    else
      dequal;
{An FAA reg requires 1 minute between departure clearances, }
{ so min idt is 1.0                    }
  if times[f,l,1] < 1 then times[f,l,1]:= 1;
{ When wake vorticies are present, must wait for 2 minutes after heavy/757 }
  if (WAKE = 1) and (l>=4) and (times[f,l,1]<2+cbar) then times[f,l,1]:= 2+cbar;
  end;  { loop for D-D-D ..... }
```

```
{Now compute average idt:}
tdd:=0;for i:=1 to nc do for j:=1 to nc do tdd:=tdd+p[i]*p[j]*times[i,j,1];
dmax:=trunc(60/tdd);
v1:=0;v2:=jmax;
writeln(ofl,v1,' ',dmax);
writeln(ofl,ad,' ',ad);
writeln(ofl,amax,' ',v2);
writeln(ofl,amax,v1);
close(ofl)
end.
```

REPORT DOCUMENTATION PAGE

Form Approved
OPM No.0704-0188

1. AGENCY USE ONLY *(Leave Blank)*	2. REPORT DATE	3. REPORT TYPE AND DATES COVERED
	April 1997	Contractor Report

4. TITLE AND SUBTITLE

Estimating the Effects of the Terminal Area Productivity Program

5. FUNDING NUMBERS

C NAS2-14361

WU 538-08-11-01

6. AUTHOR(S)

David A. Lee, Peter F. Kostiuk, Robert V. Hemm, Jr., Earl R. Wingrove, III, Gerald Shapiro

7. PERFORMING ORGANIZATION NAME(S) AND ADDRESS(ES)

Logistics Management Institute
2000 Corporate Ridge
McLean, VA 22102-7805

8. PERFORMING ORGANIZATION REPORT NUMBER

LMI– NS301T3

9. SPONSORING/MONITORING AGENCY NAME(S) AND ADDRESS(ES)

National Aeronautics and Space Administration
Langley Research Center
Hampton, VA 23681-0001

10. SPONSORING/MONITORING AGENCY REPORT NUMBER

NASA CR-201682

11. SUPPLEMENTARY NOTES

Langley Technical Monitor. Robert Yackovetsky
Final Report

12a. DISTRIBUTION/AVAILABILITY STATEMENT

Unclassified-Unlimited
Subject Category 01
Availability: NASA CASI, (301) 621-0390

12b. DISTRIBUTION CODE

13. ABSTRACT *(Maximum 200 words)*

The report describes methods and results of an analysis of the technical and economic benefits of the systems to be developed in the NASA Terminal Area Productivity (TAP) program. A runway capacity model using parameters that reflect the potential impact of the TAP technologies is described. The runway capacity model feeds airport specific models which are also described. The capacity estimates are used with a queuing model to calculate aircraft delays, and TAP benefits are determined by calculating the savings due to reduced delays. The report includes benefit estimates for Boston Logan and Detroit Wayne County airports. An appendix includes a description and listing of the runway capacity model.

14. SUBJECT TERMS	15. NUMBER OF PAGES
Aeronautics, aviation system, NASA technology, terminal area productivity, airport capacity	106
	16. PRICE CODE: A06

17. SECURITY CLASSIFICATION OF REPORT	18. SECURITY CLASSIFICATION OF THIS PAGE	19. SECURITY CLASSIFICATION OF ABSTRACT	20. LIMITATION OF ABSTRACT
Unclassified	Unclassified		UL